



**NAVAL
POSTGRADUATE
SCHOOL**

MONTEREY, CALIFORNIA

THESIS

**LOW-SPEED WIND TUNNEL FLOW
QUALITY DETERMINATION**

by

Scott A. Harvey

September 2011

Thesis Advisor:

M. S. Chandrasekhara

Second Reader:

K. D. Jones

Approved for public release; distribution is unlimited

THIS PAGE INTENTIONALLY LEFT BLANK

REPORT DOCUMENTATION PAGE			<i>Form Approved OMB No. 0704-0188</i>
Public reporting burden for this collection of information is estimated to average 1 hour per response, including the time for reviewing instruction, searching existing data sources, gathering and maintaining the data needed, and completing and reviewing the collection of information. Send comments regarding this burden estimate or any other aspect of this collection of information, including suggestions for reducing this burden, to Washington headquarters Services, Directorate for Information Operations and Reports, 1215 Jefferson Davis Highway, Suite 1204, Arlington, VA 22202-4302, and to the Office of Management and Budget, Paperwork Reduction Project (0704-0188) Washington DC 20503.			
1. AGENCY USE ONLY (Leave blank)	2. REPORT DATE September 2011	3. REPORT TYPE AND DATES COVERED Master's Thesis	
4. TITLE AND SUBTITLE Low-Speed Wind Tunnel Flow Quality Determination		5. FUNDING NUMBERS	
6. AUTHOR(S) Scott A. Harvey		8. PERFORMING ORGANIZATION REPORT NUMBER	
7. PERFORMING ORGANIZATION NAME(S) AND ADDRESS(ES) Naval Postgraduate School Monterey, CA 93943-5000		10. SPONSORING/MONITORING AGENCY REPORT NUMBER	
9. SPONSORING /MONITORING AGENCY NAME(S) AND ADDRESS(ES) N/A		11. SUPPLEMENTARY NOTES The views expressed in this thesis are those of the author and do not reflect the official policy or position of the Department of Defense or the U.S. Government. IRB Protocol number <u> N/A </u> .	
12a. DISTRIBUTION / AVAILABILITY STATEMENT Approved for public release; distribution is unlimited		12b. DISTRIBUTION CODE A	
13. ABSTRACT (maximum 200 words) The NPS MAE wind tunnel was reinstalled, calibrated, and its flow characteristics evaluated to determine its suitability for research and classroom demonstration. The calibration involved determining tunnel speed vs. motor speed, wall static pressure distribution, total pressures across selected planes, the uniformity of the velocity profile, using a pitot-static tube and a single component hot wire (CTA), the wall boundary layer characteristics consisting of the velocity profile, streamwise turbulence intensity, and spectral energy distributions at selected points. Incorporated instrumentation includes pressure transducers attached to a pitot-static tube, wall static pressure taps, and a pressure rake; a hotwire anemometry system, and a linear traverse system. These were integrated with a data acquisition (DAQ) processor with analog to digital conversion and digital I/O boards, and controlled using in-house developed LabVIEW software. Testing showed a maximum axial velocity of 38 m/s, which is 84% of the tunnel's rated speed. The 2-D flow uniformity was within $\pm 7\%$ by pressure rake, and $\pm 3\%$ with a turbulence intensity $\approx 0.11\%$ at full speed using a CTA, affirming the tunnel's viability as a demonstration platform. Spectral density plots in the boundary layer exhibit typical behavior of fully developed equilibrium turbulent flow with an inertial sub-range present. Future testing of a flat-plate wake for drag modification is planned.			
14. SUBJECT TERMS National Instruments, LabVIEW, Virtual Instrument, Wind Tunnel, Data Acquisition, Plint, Microstar, Turbulence Intensity, Boundary Layer, Power Spectrum			15. NUMBER OF PAGES 101
			16. PRICE CODE
17. SECURITY CLASSIFICATION OF REPORT Unclassified	18. SECURITY CLASSIFICATION OF THIS PAGE Unclassified	19. SECURITY CLASSIFICATION OF ABSTRACT Unclassified	20. LIMITATION OF ABSTRACT UU

THIS PAGE INTENTIONALLY LEFT BLANK

Approved for public release; distribution is unlimited

LOW-SPEED WIND TUNNEL FLOW QUALITY DETERMINATION

Scott A. Harvey
Lieutenant, United States Navy
B.S., Auburn University, 2004

Submitted in partial fulfillment of the
requirements for the degree of

MASTER OF SCIENCE IN MECHANICAL ENGINEERING

from the

**NAVAL POSTGRADUATE SCHOOL
September 2011**

Author: Scott A. Harvey

Approved by: Muguru S. Chandrasekhara
Thesis Advisor

Kevin D. Jones
Second Reader

Knox T. Millsaps
Chair, Department of Mechanical and Aerospace Engineering

THIS PAGE INTENTIONALLY LEFT BLANK

ABSTRACT

The NPS MAE wind tunnel was reinstalled, calibrated, and its flow characteristics evaluated to determine its suitability for research and classroom demonstration. The calibration involved determining tunnel speed vs. motor speed, wall static pressure distribution, total pressures across selected planes, the uniformity of the velocity profile, using a pitot-static tube and a single component constant temperature anemometer (CTA), the wall boundary layer characteristics consisting of the velocity profile, streamwise turbulence intensity, and spectral energy distributions at selected points. Incorporated instrumentation includes pressure transducers attached to a pitot-static tube, wall static pressure taps, and a pressure rake; a hotwire anemometry system, and a linear traverse system. These were integrated with a data acquisition (DAQ) processor with analog to digital conversion and digital I/O boards, and controlled using in-house developed LabVIEW software. Testing showed a maximum axial velocity of 38 m/s, which is 84% of the tunnel's rated speed. The 2-D flow uniformity was within $\pm 7\%$ by pressure rake, and $\pm 3\%$ with a turbulence intensity $\approx 0.11\%$ at full speed using a CTA, affirming the tunnel's viability as a demonstration platform. Spectral density plots in the boundary layer exhibit typical behavior of fully developed equilibrium turbulent flow with an inertial sub-range present. Future testing of a flat-plate wake for drag modification is planned.

THIS PAGE INTENTIONALLY LEFT BLANK

TABLE OF CONTENTS

I.	INTRODUCTION.....	1
II.	FACILITY DESCRIPTION	3
A.	WIND TUNNEL.....	3
B.	DATA ACQUISITION SYSTEM	5
	1. Microstar Hardware System.....	6
	<i>a. Microstar Industrial Enclosure 012-06-P</i>	<i>6</i>
	<i>b. Microstar Digital Expansion Board MSXB 038-09-E3C-</i> <i>B.....</i>	<i>6</i>
	<i>c. Microstar Expansion Board MSXB 048-03-25K-E2C-B.....</i>	<i>8</i>
	<i>d. Microstar Data Acquisition Processor 5200a/626</i>	<i>8</i>
C.	DELL PRECISION T5500 32-BIT WORKSTATION	9
	1. Windows 7, 32-bit.....	9
	2. Power Supply.....	10
	3. PCI Slots	10
	<i>a. PCI-x.....</i>	<i>10</i>
	<i>b. PCI-e.....</i>	<i>10</i>
	<i>c. PCI.....</i>	<i>10</i>
D.	SENSORS AND INSTRUMENTATION	11
	1. Scanivalve Digital Sensor Array DSA 3217.....	11
	2. Pressure Sensing Tubes	12
	<i>a. Pitot-static Tube</i>	<i>12</i>
	<i>b. Boundary Layer Probe.....</i>	<i>13</i>
	<i>c. Pressure Rake.....</i>	<i>13</i>
	3. MKS Baratron Pressure Measuring Equipment	14
	<i>a. PR4000F.....</i>	<i>14</i>
	<i>b. 223B Differential Pressure Transducer.....</i>	<i>16</i>
	<i>c. 750B Absolute Pressure Transducer.....</i>	<i>16</i>
	4. Inclined Manometer.....	17
	5. Hot Wire Anemometry (HWA/CTA) System.....	17
	<i>a. Cable Length, S3.....</i>	<i>18</i>
	<i>b. Gain, S4.....</i>	<i>18</i>
	<i>c. Filter, S5.....</i>	<i>18</i>
	<i>d. Shape, S6.....</i>	<i>18</i>
E.	VELMEX BISLIDE TRAVERSING ASSEMBLY	19
	1. BiSlide Unit.....	19
	2. Traverse Motor	19
	3. VP9000 Stepper Motor Controller	20
F.	DATA ACQUISITION AND PROCESSING PACKETS	21
	1. DSALink3	21
	2. Data Acquisition Programming Language, DAPL 2000	21
	3. LabVIEW.....	22
	<i>a. DSA 3217.....</i>	<i>23</i>

	b.	<i>Data Acquisition Processor</i>	24
	c.	<i>Velmex BiSlide</i>	26
	4.	MATLAB	27
III.		EXPERIMENTAL PROCEDURES AND RESULTS	29
	A.	WIND TUNNEL CALIBRATION	29
	1.	Test Setup	29
	a.	<i>Pitot-Static Tube</i>	29
	b.	<i>DSA 3217 Connection</i>	29
	c.	<i>Wind Tunnel Warm Up</i>	31
	d.	<i>DSA 3217 CalZero</i>	32
	e.	<i>DSA 3217 VI Setup</i>	34
	f.	<i>Establish Initial Conditions</i>	35
	2.	Conduct of Testing	35
	a.	<i>Data Collection</i>	35
	b.	<i>Securing the Wind Tunnel</i>	35
	3.	Tunnel Speed Calculation	36
	a.	<i>Data Transfer</i>	36
	b.	<i>Determining Tunnel Speed</i>	36
	4.	Calibration Results	37
	a.	<i>Problems and Resolutions</i>	37
	b.	<i>Tunnel Speed Results</i>	38
	B.	2-D VELOCITY MAPPING	39
	1.	Test Setup	39
	a.	<i>Pressure Rake installation</i>	39
	b.	<i>Instrument Setup and Tunnel Warmup</i>	40
	2.	Conduct of Testing	40
	a.	<i>Data Collection</i>	40
	b.	<i>Securing the Wind Tunnel</i>	41
	c.	<i>Data Processing</i>	41
	3.	2-D Mapping Results	42
	C.	WALL STATIC PRESSURE DISTRIBUTION MAPPING	43
	1.	Test Setup	43
	a.	<i>Tunnel Setup</i>	43
	b.	<i>Instrument Setup and Tunnel Warmup</i>	44
	2.	Conduct of Testing	44
	a.	<i>Data Collection</i>	44
	b.	<i>Securing the Wind Tunnel</i>	44
	c.	<i>Data Processing</i>	44
	3.	Wall Static Pressure Profile	45
	a.	<i>Wall Static Pressure with Open Vent</i>	45
	b.	<i>Wall Static Pressure with Taped Vent</i>	47
	c.	<i>Comparison</i>	48
	D.	CTA/BOUNDARY LAYER PROBE TRAVERSAL	49
	1.	CTA Calibration	49
	a.	<i>CTA Setup</i>	49

	<i>b.</i>	<i>CTA Balancing</i>	52
	<i>c.</i>	<i>CTA Resistance Measurement</i>	52
	<i>d.</i>	<i>Overheat Selection</i>	53
	<i>e.</i>	<i>Square Wave Response Check</i>	54
2.		Test Setup	55
	<i>a.</i>	<i>Tunnel Setup</i>	55
	<i>b.</i>	<i>Instrument Setup and Tunnel Warmup</i>	57
3.		CTA Calibration Coefficient Determination	58
	<i>a.</i>	<i>Data Collection</i>	58
	<i>b.</i>	<i>Data Processing</i>	60
4.		Boundary Layer Measurement	62
	<i>a.</i>	<i>Data Collection</i>	62
	<i>b.</i>	<i>Data Processing</i>	63
5.		CTA Calibration Verification	63
	<i>a.</i>	<i>Data Collection</i>	63
	<i>b.</i>	<i>Securing the Wind Tunnel</i>	64
	<i>c.</i>	<i>Data Processing</i>	64
6.		CTA Test Results	64
	<i>a.</i>	<i>CTA Velocity</i>	64
	<i>b.</i>	<i>Turbulence Intensity</i>	66
	<i>c.</i>	<i>Boundary Layer</i>	67
	<i>d.</i>	<i>Spectral Density</i>	68
IV.		CONCLUDING REMARKS AND RECOMMENDATIONS	73
	A.	REMARKS	73
		1. Velocity Characteristics	73
		2. Turbulence Intensity	73
		3. Boundary Layer Characteristics	73
	B.	RECOMMENDATIONS	74
		1. Wind Tunnel Disassembly	74
		2. Conduct of Testing	74
	C.	CONCLUSION	75
		BIBLIOGRAPHY	77
		LIST OF REFERENCES	79
		INITIAL DISTRIBUTION LIST	81

THIS PAGE INTENTIONALLY LEFT BLANK

LIST OF FIGURES

Figure 1.	Laboratory Setup.....	3
Figure 2.	Halligan Hall Low-Speed Wind Tunnel	4
Figure 3.	Test Section Diagram, with Static Pressure Tap Locations	5
Figure 4.	Wall Static Pressure Plugs	5
Figure 5.	MSXB 038 Configuration Diagram Example (After Microstar, 2003).....	7
Figure 6.	Data Acquisition System Diagram (After Microstar, 2011).....	9
Figure 7.	Scanivalve DSA 3217 (From Scanivalve, 2011)	11
Figure 8.	Pitot-static Tube (From United Sensor, 2011).....	12
Figure 9.	Boundary Layer Probe (From United Sensor, 2011).....	13
Figure 10.	Pressure Rake.....	14
Figure 11.	PR4000 Front and Back Panels (After MKS, 2000).....	15
Figure 12.	CTA Bridge Internal Switches (From Dantec, 2003).....	17
Figure 13.	BiSlide Traverse Assembly (From Velmex, 2011).....	19
Figure 14.	VP9000 Stepper Motor Controller.....	20
Figure 15.	DAPL Architecture (After Microstar, 2011)	22
Figure 16.	DSA 3217 LabVIEW Front Panel	24
Figure 17.	DAP LabVIEW Code	25
Figure 18.	DAP LabVIEW Front Panel	26
Figure 19.	BiSlide LabVIEW Code	27
Figure 20.	MATLAB Power Spectrum Code.....	28
Figure 21.	Connecting to DSA 3217	30
Figure 22.	Internet Address Entry for DSA 3217	31
Figure 23.	Wind Tunnel Control Panel	32
Figure 24.	Connecting to DSA 3217	33
Figure 25.	Verifying DSALink Connection.....	33
Figure 26.	DSALink CalZero Response.....	34
Figure 27.	Velocity Template (example)	36
Figure 28.	MKS Baratron and DSA 3217 Indicated Pressure Differences	37
Figure 29.	Tunnel Speed Comparison by Sensor Type.....	38
Figure 30.	Test Section Tunnel Speed vs. Speed Dial Position	39
Figure 31.	2-D Velocity Template (example)	41
Figure 32.	2-D Relative Velocity Profile	43
Figure 33.	Wall Static Pressure Template (example).....	45
Figure 34.	Wall Static Pressure, Vented Test Section, Fan Access Gasket Installed	46
Figure 35.	Wall Static Pressure, Vented Test Section, Fan Access Gasket Removed	47
Figure 36.	Wall Static Pressure, Sealed Test Section, Fan Access Gasket Removed.....	48
Figure 37.	Wall Static Pressure Distribution Comparison	49
Figure 38.	CTA Bridge and CTA Front Panel (From DANTEC, 2003).....	50
Figure 39.	CTA Signal Conditioner	51
Figure 40.	CTA RMS and Mean Value.....	51
Figure 41.	CTA Square Wave Response (From DANTEC, 2003)	54
Figure 42.	Incorrect CTA Square Wave Responses (After DANTEC, 2003)	55

Figure 43.	DAP Setup	57
Figure 44.	DAP Data Acquired	58
Figure 45.	DAP Data Saved	59
Figure 46.	Velmex Command Entry for Boundary Layer Initial Conditions	60
Figure 47.	CTA Plot (E vs U).....	61
Figure 48.	CTA Linearized Calibration Plot (E^2 vs \sqrt{U}).....	61
Figure 49.	CTA Post Test Comparison with 60 Minute Tunnel Warm-up.....	65
Figure 50.	CTA Post Test Comparison with Insufficient Tunnel Warm-up.....	65
Figure 51.	Average Tunnel Turbulence Intensity	67
Figure 52.	Boundary Layer Profile.....	68
Figure 53.	Sine Wave Spectral Density.....	69
Figure 54.	Freestream Spectral Density	70
Figure 55.	Boundary Layer Spectral Density (2mm from wall)	71

LIST OF TABLES

Table 1. MSXB 038 BNC Connector Map.....7
Table 2. MKS 223B Wiring Diagram (From MKS, 1999).....16

THIS PAGE INTENTIONALLY LEFT BLANK

LIST OF ACRONYMS AND ABBREVIATIONS

δ	Boundary Layer Thickness
δ^*	Displacement Thickness
μ	Dynamic Viscosity of Air (lbf-s/ft ²)
μV	Microvolts
θ	Momentum Thickness
BNC	Bayonet Neill-Concelman
C	Celsius
CTA	Constant Temperature Anemometer
DAP	Data Acquisition Processor
DAPL	Data Acquisition Programming Language
DoD	Department of Defense
E	Voltage
F	Fahrenheit
GB	Gigabyte
GHz	Gigahertz
Hz	Hertz
ID	Inside Diameter
I/O	Input/Output
kHz	Kilohertz
kW	Kilowatt
LT	Lieutenant
M	Mach Number
MAE	Mechanical and Aerospace Engineering
MB	Megabyte
MSIE	Microstar Industrial Enclosure
MSXB 038	16 Channel, Digital Input/Output Expansion Board
MSXB 048	16 Channel, Filtered Analog Input Board
NI	National Instruments
NPS	Naval Postgraduate School

OD	Outside Diameter
p	Static Pressure (psi)
P_o	Stagnation Pressure (psi)
PC	Dell Precision T5500 32-bit Workstation
PCI	Peripheral Component Interconnect
psia	pounds force per square inch (absolute)
psid	pounds force per square inch (differential)
PST	Pitot-static Tube
RAM	Random Access Memory
Re	Reynolds number
T	Ambient Temperature (F)
U_∞	Freestream Tunnel Velocity (m/s)
U_{CTA}	Local CTA Velocity (m/s)
V	Volt
VI	Virtual Instrument
W	Watt

ACKNOWLEDGMENTS

I would like thank the following personnel for their assistance and guidance during this endeavor. First, to my thesis advisor, Professor Muguru Chandrasekhara, for his invaluable knowledge regarding wind tunnel testing and fluid dynamics general, and particularly for his supportive attitude and guidance during the difficult times where it looked like I would never finish. Thank you also to Dr. Michael Wilder from NASA Ames Research Center, without his counsel the data acquisition system would never have gotten off the ground. To Douglas Seivwright at NPS, who sacrificed his time to assist me in the instrumentation and control of the array of sensors necessary to complete this endeavor; without his expertise in LabVIEW programming integration of software and hardware for data acquisition would not have been possible. Thank you goes to John Mobley and his model making team, for the manufacture of many innovative parts to enable many of the experiments performed. Thanks to Milan Vukceovich, who assisted in the setup of and installation of software on the computer used to run the lab. For all their help in configuring the Microstar hardware, I would like to thank Kristin Bunzel and the Microstar's support staff for their quick response in answering my questions and resolving any issues I had. Finally, and most of all, thank you to my wife, Fancy, and my children; without their patience, love, and support I would not have been able to finish this thesis and complete my master's degree.

THIS PAGE INTENTIONALLY LEFT BLANK

I. INTRODUCTION

Low speed ($M \leq \sim 0.3$) wind tunnel testing continues to play an important role in fluid mechanics, aerodynamics, and in validating results from numerical simulations using computational fluid dynamics (CFD). A tremendous increase in computational power has allowed simulations that were, until recently, not possible to pursue, and while these simulations yield a greater insight into the realm of fluid dynamics through modeling, the experimental verification of these simulations and models in laboratory wind tunnels which corroborate the findings in a physically verifiable and repeatable manner is still necessary. These laboratory facilities must be thoughtfully constructed, in order to adequately measure, record, and process the data from these parameters in order to fully describe the flow within the test section. Models inserted in wind tunnels generate flows with the complexities inherent to fluid dynamics. Quantifying relevant flow quantities such as the tunnel speed, Reynolds number, turbulence intensity, boundary layer thickness the drag coefficients of specimens are integral to the engineering design factors such as performance, procurement and operational cost, platform stability, and many other facets which a customer may require.¹ For low speed wind tunnels, matching the key similarity parameter of Reynolds number on a fixed geometry model allows scaling of experimental results for various physical dimensions and properties of different fluids. It is the potential scalability of results that makes wind tunnel testing an essential, viable tool in fluid mechanics. Although many times, perfect dynamic similarity (Reynolds number matching) may be elusive, the fact that many design parameters are only weak functions of Reynolds number makes a wind tunnel a very useful tool for the aerodynamicist. Determining the drag and other performance coefficients and associated drag force on a model, and developing methods to reduce these values is of vital importance in the fiscal and operational arenas of sea or air vehicles. For example, straight riblets have been proven to reduce drag by 5–6%, even in flight tests. Thus, they appear attractive for ship hull drag reduction which needs to be

¹ Jewel Barlow, William Rae, and Alan Pope, *Low-Speed Wind Tunnel Testing* (Wiley-Interscience, 1999), 46.

studied in detail. In order to adequately isolate the extraneous interference effects of the presence of the model inside a wind tunnel (blockage), and to faithfully simulate free flight conditions, it is important to monitor various parameters pertinent to the flow quality (uniformity, turbulence levels, spectral content, blockage) and wall pressure field characterization of the empty test section must first be documented so that the effects on any potential model in a tunnel may be evaluated.

To meet this testing need at NPS and to establish a state of the art test facility, a Plint TE44 wind tunnel was reassembled in the basement of MAE department Halligan Hall after being held in storage for over a decade. The wind tunnel has been set up with a set of sensors and instrumentation, integrated with a data acquisition system, and run to evaluate its operating characteristics, overall health, and potential for research and in-class laboratory use. The first task was to install and verify the calibration of the requisite instrumentation and DAQ boards used to certify the wind tunnel, write and debug the software codes for data acquisition and processing, and establish the ability to communicate between the sensors and control them from the host computer (PC). After verifying the system setup, the wind tunnel was operated under different operating modes in order to obtain a tunnel speed calibration versus fan speed and determine the flow characteristics. Since the tunnel is vented at the aft end of the test section, it was necessary to appraise the ability of the tunnel to function as a suitable applied aerodynamics test bed by measuring the wall static pressure distribution and turbulence intensity in the test section. Tests on a flat-plate are planned for the near future with the aim of measuring the drag force on the plate, and subsequently explore methods to reduce it using non-standard means, such as riblets attached to the flat plate surface, to determine the effects on the turbulent boundary layer and modification on the drag. The latter effort offers the potential to explore reducing the hull drag of surface ships.

II. FACILITY DESCRIPTION

The wind tunnel and all associated equipment are located in the basement of Halligan Hall, Room 031A (Figure 1).



Figure 1. Laboratory Setup

A. WIND TUNNEL

The NPS MAE wind tunnel (Figure 2) is a horizontally mounted, closed circuit, subsonic model TE44 wind tunnel driven by an 11kW DC, variable speed, axial flow fan manufactured by Plint and Partners, Ltd. The ducting is constructed of sheet steel with turning vanes installed at each corner. The flow passes through a 7.3:1 contraction cone immediately before entering the 457 mm x 457 mm test section. Corner fillets are present in both the contraction cone and the test section to smooth out corner flow and provide a uniform longitudinal pressure distribution along the 1,200 mm test section.²

²Ibid., 96.

The test section is accessible by an acrylic glass window on each side of the wind tunnel. Immediately following the test section, the air passes through a vented section, into the diffuser section, and returns to the fan inlet.

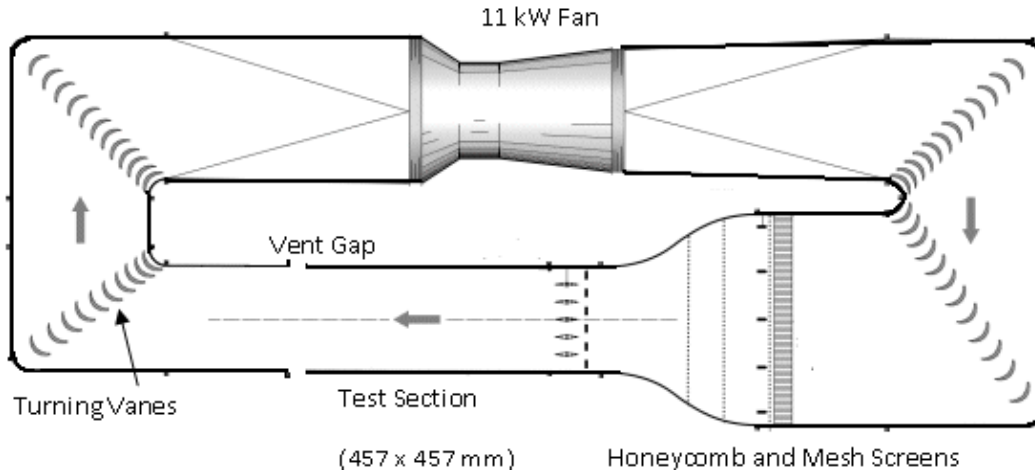


Figure 2. Halligan Hall Low-Speed Wind Tunnel

The test section is fitted with nine static pressure ports (Figure 3) along the dorsal centerline for measuring the wall static pressure distribution. Each port has a plastic, fitted plug with a 0.063” pressure sensing tube that sits flush with the top of the test section inner wall and a tube protruding two inches from the top of the plug to allow a connection to the DSA 3217 via 0.063” tubing (Figure 4). The first static pressure port, labeled as Position 0, located at the entrance to the test section is fitted with a pitot-static tube for the tunnel freestream velocity measurement (Paragraph C.2.a). The contraction section also has two ports for tunnel speed calculation at its ends where the flow is not accelerating.

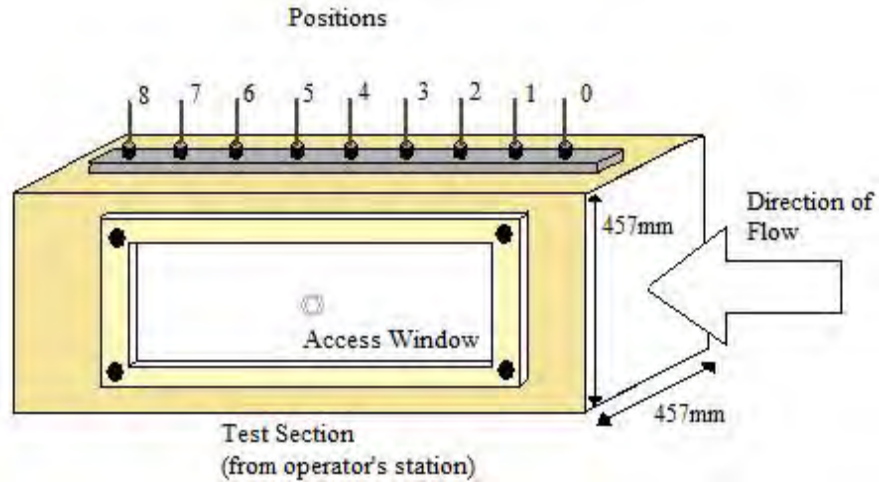


Figure 3. Test Section Diagram, with Static Pressure Tap Locations



Figure 4. Wall Static Pressure Plugs

B. DATA ACQUISITION SYSTEM

The data acquisition (DAQ) system for the MAE wind tunnel consists of four major subsystems: a Dell PC, Microstar circuit boards (both analog to digital I/O and digital input boards), a collection of sensors including pressure transducers and single component, constant temperature anemometers, and a software suite for data collection and processing including LabVIEW, MATLAB, and Excel.

1. Microstar Hardware System

a. Microstar Industrial Enclosure 012–06-P

In an effort to integrate the range of boards used in the experiment, and simplify the transferring of the signals to the data acquisition boards, the method recommended by Microstar of using the Microstar Industrial Enclosure, MSIE 012–06-P was used. The MSIE is a full-sized (19”), rack-mounted chassis housing a half analog/half digital backplane for use with Microstar expansion boards in data acquisition applications. Each side of the enclosure is capable of holding ten expansion boards with two 36” shielded cables connecting the boards within the MSIE to the DAP contained within the PC to ensure high signal quality and minimize electrical noise from the environment.

b. Microstar Digital Expansion Board MSXB 038–09-E3C-B

The MSXB 038 digital expansion board (Figure 5) provides the Data Acquisition Processor (DAP) with 16 channels each of digital inputs and digital outputs.³ Each BNC jack has a signal and a ground cable soldered to the connector with the free end available to plug into Wago terminal connectors on the MSXB 038 board. The current configuration of the hardware has been set up to provide eight digital (differential) inputs and outputs via BNC connectors (Table 1). The MSXB 038 communicates to the DAP through the digital backplane of the MSIE and the MSCBL 054–01-L36 shielded cable.

³ Microstar Laboratories, Inc., *MSXB 038 Accessory Board Manual* (Microstar Laboratories, Inc., 2003), 1–6.

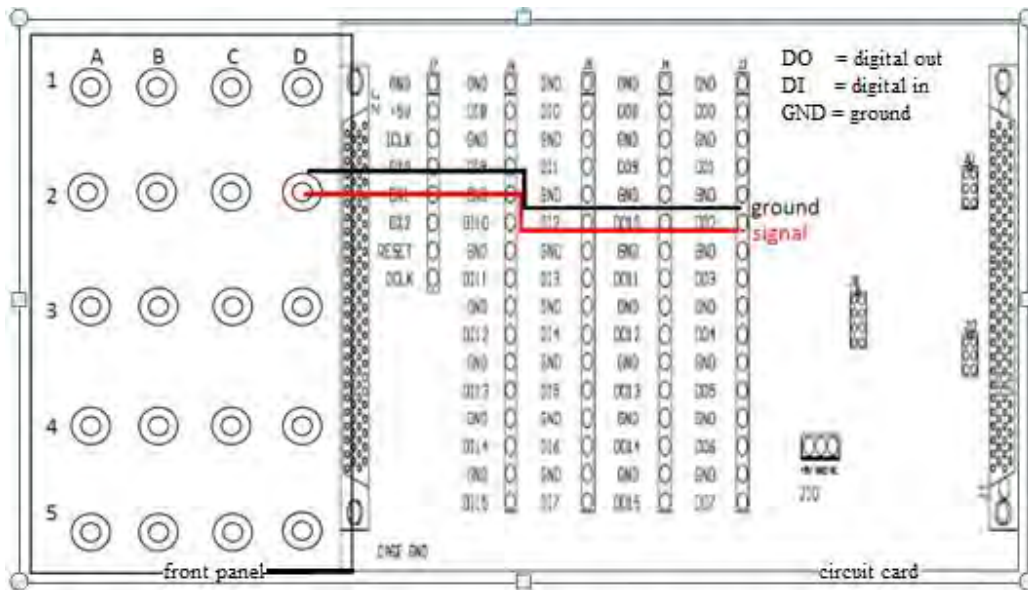


Figure 5. MSXB 038 Configuration Diagram Example (After Microstar, 2003)⁴

Front Panel BNC Jack Number	Wago Terminal Address	Front Panel BNC Jack Number	Wago Terminal Address
1A	DI0	1C	DO0
2A	DI1	2C	DO1
3A	DI2	3C	DO2
4A	DI3	4C	DO3
5A	DI4	5C	DO4
1B	DI5	1D	DO5
2B	DI6	2D	DO6
3B	DI7	3D	DO7
4B	DI8	4D	DO8
5B	DI9	5D	DO9
not used	DI10	not used	DO10
not used	DI11	not used	DO11
not used	DI12	not used	DO12
not used	DI13	not used	DO13
not used	DI14	not used	DO14
not used	DI15	not used	DO15

Table 1. MSXB 038 BNC Connector Map

⁴ Ibid., 3.

c. *Microstar Expansion Board MSXB 048-03-25K-E2C-B*

The MSXB 048 is a 16 channel, filtered, analog input expansion board. Inputs are via BNC connectors on the front panel of the MSIE and the outputs are sent to the DAP via the analog backplane of the MSIE and the MSCBL 040-01-L36 cable. Each channel has a four-pole, low-pass Butterworth filter with a cutoff frequency of 25 kHz. Microstar's stated gain error of the MSXB 048 is typically less than 0.012% with a maximum error of 0.019%.

d. *Microstar Data Acquisition Processor 5200a/626*

The Data Acquisition Processor (DAP) system consists of two electronic boards installed within the PC. The primary board is a high-speed data acquisition processor that occupies one PCI-x slot in the PC and is connected to the secondary MSCBL 076 board occupying a PCI-e slot and communicates with the DAP via a 100-pin ribbon cable (Figure 6). The DAP has a tall heat sink and fan to meet the cooling requirements of the on board processor; no card may be inserted next to the DAP if it interferes with the heat sink.⁵ Insufficient air flow across the heat sink can cause damage to the DAP. The analog input signal range to the DAP is ± 10 V, providing a 14-bit accuracy with a maximum sampling rate of 417,000 samples/second/channel with a voltage resolution of 1.2 mV. This is sufficient resolution to measure turbulence intensities of 0.1% or less.

⁵ Microstar Laboratories, Inc., *DAP 5200a Manual* (Microstar Laboratories, Inc., 2001), 4.

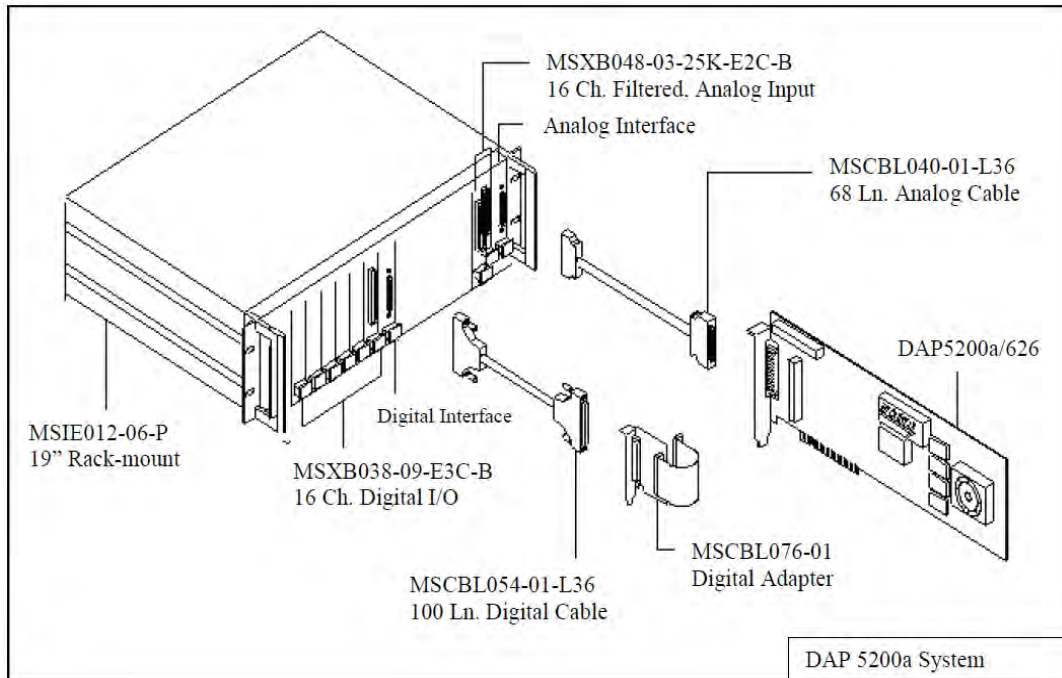


Figure 6. Data Acquisition System Diagram (After Microstar, 2011)⁶

C. DELL PRECISION T5500 32-BIT WORKSTATION

A customized Dell T5500 desktop is configured to meet the specific needs of both the hardware and software of the data acquisition system and its associated peripherals. The PC has a dual core processor running at 2 GHz with 4 GB of RAM to ensure the PC exceeds the minimum RAM requirements for running the DAPL, DSALink3, and LabVIEW software suites to gather data while still allowing enough processing power for Excel and MATLAB to execute data processing routines. The capability of the 512 MB graphics card exceeds the minimum requirements for LabVIEW and provides the user with a dual screen capability with the requisite 1024 x 768 pixel resolution for operating the NI software.

1. Windows 7, 32-bit

Windows 7 is the primary operating system on Dell computers. The 32-bit operating system was selected because of its compatibility with both Microstar

⁶ Microstar Laboratories, Inc., <http://www.mstarlabs.com/dataacquisition/graphics/dap5200adrawing.html>, accessed 6 September 2011.

DSALink3 and DAPL software suites which facilitate communication between the Microstar boards, the host PC, and the DSA 3217 pressure sensor.

2. Power Supply

An oversized, 1000W power supply and larger heat sink are integrated into the PC to meet the minimum power requirements to operate the PC hardware and fulfill the 30W power demand of the two DAP boards while maintaining the PC below its maximum operating temperature of 95°F.

3. PCI Slots

a. PCI-x

One 188 pin connection in a full length PCI-x card slot is reserved for the data acquisition processor (DAP). The DAP is wider than a normal PCI card due to the heat sink, and required the adjacent card to be removed in order for the DAP to fit inside the PC enclosure. The removal of the adjacent card removes the 1394 serial bus interface (Firewire) capability of the PC.

b. PCI-e

Two of the three PCI-e slots within the PC are occupied by the graphics card and the digital card of the DAP. The digital MSXB 038 card is connected to the analog card via the MSCBL076–01 cable (Figure 4) and occupies a PCI-e slot for stability and ease of access.

c. PCI

A two port serial PCI card occupies the single PCI slot within the PC. The serial ports allow communication between an MKS PR4000 pressure transducer power supply and display unit, a Velmex BiSlide traverse motor controller, and the PC.

D. SENSORS AND INSTRUMENTATION

1. Scanivalve Digital Sensor Array DSA 3217

The Scanivalve DSA 3217 incorporates 16 temperature compensated piezo-resistive pressure sensors with a pneumatic calibration valve, RAM, 16 bit A/D converter, and a microprocessor in one housing unit (Figure 7). The sensor has a range of ± 1 psid and an accuracy of 0.12% of full scale and is set up to use Ethernet (10baseT) communication with the host computer via TCP/IP protocol interface with LabVIEW at a maximum scan rate of 500 Hz/channel.⁷ The pressures measured by the DSA 3217 are temperature compensated over a range of 0°C to 60°C with a maximum thermal error of $\pm 0.001\%$ of full scale/°C, eliminating the need for temperature compensation on recorded data.

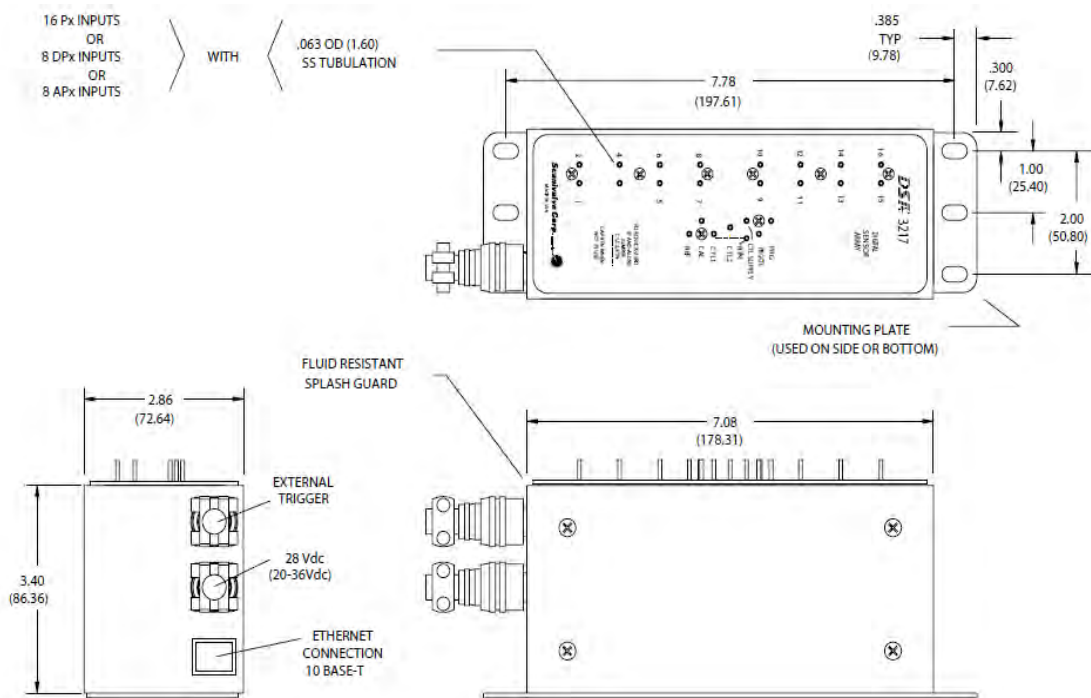


Figure 7. Scanivalve DSA 3217 (From Scanivalve, 2011)⁸

⁷ Scanivalve Corporation, http://www.instrumentation.it/main/pdf/scanivalve/prod_dsa3217_18_03-11_ID.pdf, accessed 6 September 2011.

⁸Ibid.

2. Pressure Sensing Tubes

a. Pitot-static Tube

A customized pitot-static tube (PST) (Model PAA-8-KL) was manufactured by United Sensor Corporation for measuring static and total pressure in the wind tunnel test section for the purpose of determining tunnel speed (Figure 8). The device is composed of a 0.065" stainless steel tube with an inner diameter of 0.016" for total pressure measurement, and four 0.014" ports for static pressure. Due to the small sensing port size of the PST and tubing to the Scanivalve pressure brick, there is a very slow frequency response to a change in conditions within the test section, on the order of four minutes to allow pressure equalization. The arm length of the pitot tube is adjustable via a Teflon impregnated ferrule up to its maximum length of eight inches, allowing it to be fixed at any point along its length.

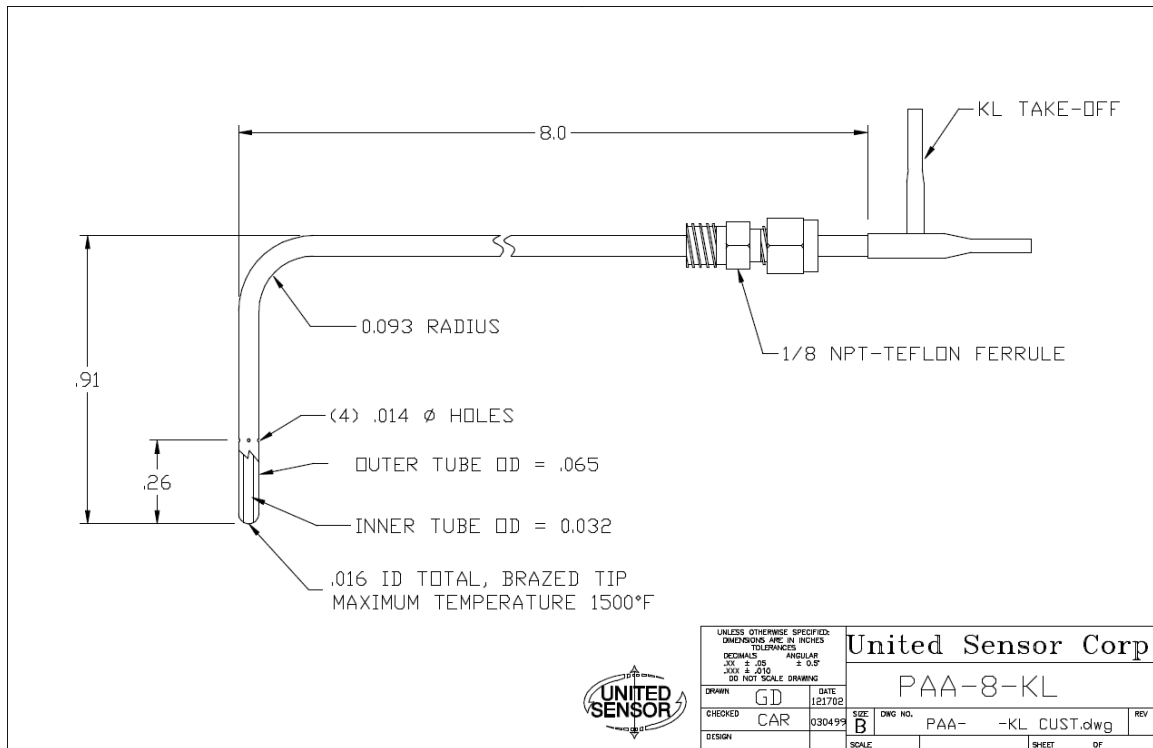


Figure 8. Pitot-static Tube (From United Sensor, 2011)⁹

⁹ United Sensor Corporation, *Drawing No. PAA-8-KL* (United Sensor Corp., 2011), 1.

b. Boundary Layer Probe

A customized boundary layer probe (Model BR-025-24-C-23-120) was manufactured by United Sensor Corporation for measuring total pressure near a fluid-solid interface such as the wall of the test section (Figure 9). The probe is 24” long with a 23” fairing to provide rigidity for measuring pressures across the test section. The sensing head of the probe is a flattened 0.025” port to yield measurements very close to the walls.

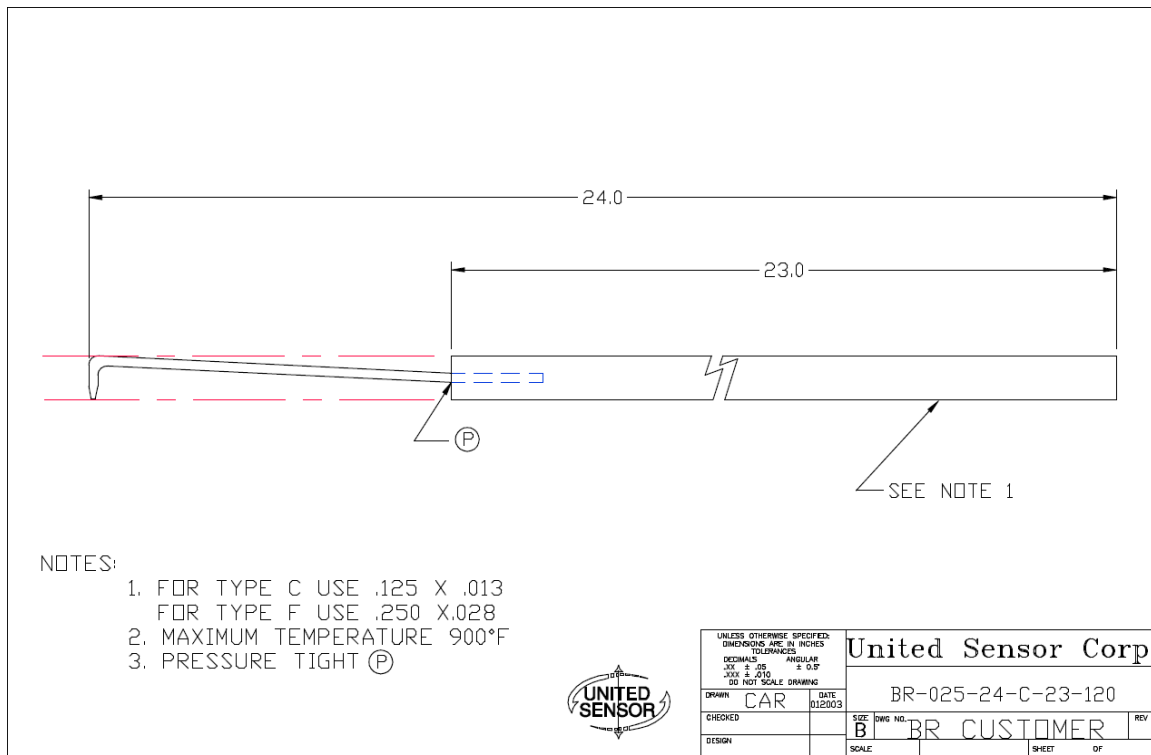


Figure 9. Boundary Layer Probe (From United Sensor, 2011)¹⁰

c. Pressure Rake

A customized pressure rake was designed in-house and manufactured in order to acquire data for the development of a two-dimensional cross sectional flow representation within the test section (Figure 10). The pressure rake consists of thirteen 0.065” O.D., stainless steel tubes mounted on a 1.5 inch I.D. PVC pipe cut to a length of

¹⁰ United Sensor Corporation, *Drawing No. BR-025-25-C-23-120* (United Sensor Corp., 2011), 1.

17.5.” The tubes closest to the ends of the PVC pipe are 0.5” from the end of the PVC pipe and the remaining probes are mounted one inch apart such that the central (seventh) tube is aligned with the test section centerline and end tubes are one inch from the upper and lower test section walls. The pressure sensing tubes extend two inches from the front of the PVC pipe to minimize upstream interference effects from the PVC pipe on the sensors. The pressure rake detectors connect to the DSA 3217 via 0.063” inside diameter tubing, and a similar four minute stabilization time is required as on the PST. A ½” stud was inserted perpendicular to the PVC pipe to rigidly mount the pressure rake and provide a means of traverse control within the test section.

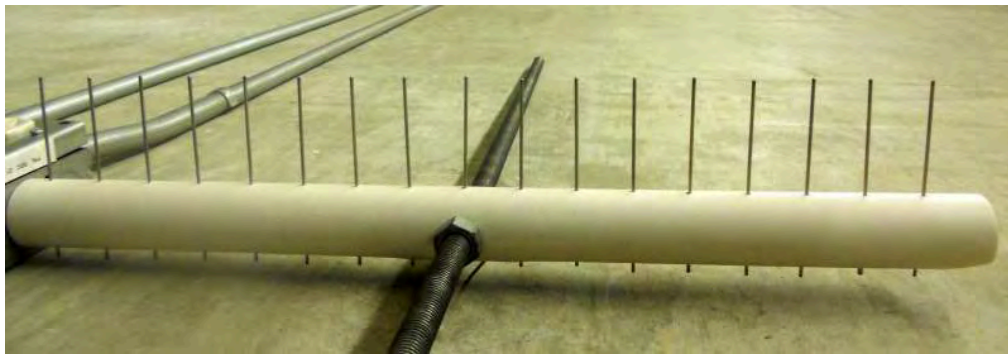


Figure 10. Pressure Rake

3. MKS Baratron Pressure Measuring Equipment

a. *PR4000F*

The PR4000F control unit is a dual channel power supply control unit with a digital readout capable of displaying multichannel signals and setpoints. Each signal channel, setpoint or relay can be programmed by the user and set to display with a user selected, preprogrammed engineering units. The current configuration is set to read two channels of pressure in centimeters of water with: Channel 1 displaying differential pressure from the Type 223B transducer, and Channel 2 reading absolute pressure from the Type 750B. Each channel’s input and output voltage, type of units, setpoints and range must be set by the user as required by the appropriate sensors’ technical manuals. Sensors are attached via RS232 cables to Channels 1 and 2 on the back panel of the control unit; additional RS232 connections are available to connect triggering hardware,

relays and to transmit the processed data from the PR4000F to the DAP in the PC via the 2-port serial board (Figure 11). The PR4000F and attached sensors should be energized and warmed up for at least one hour prior to use to minimize errors due to thermal effects.

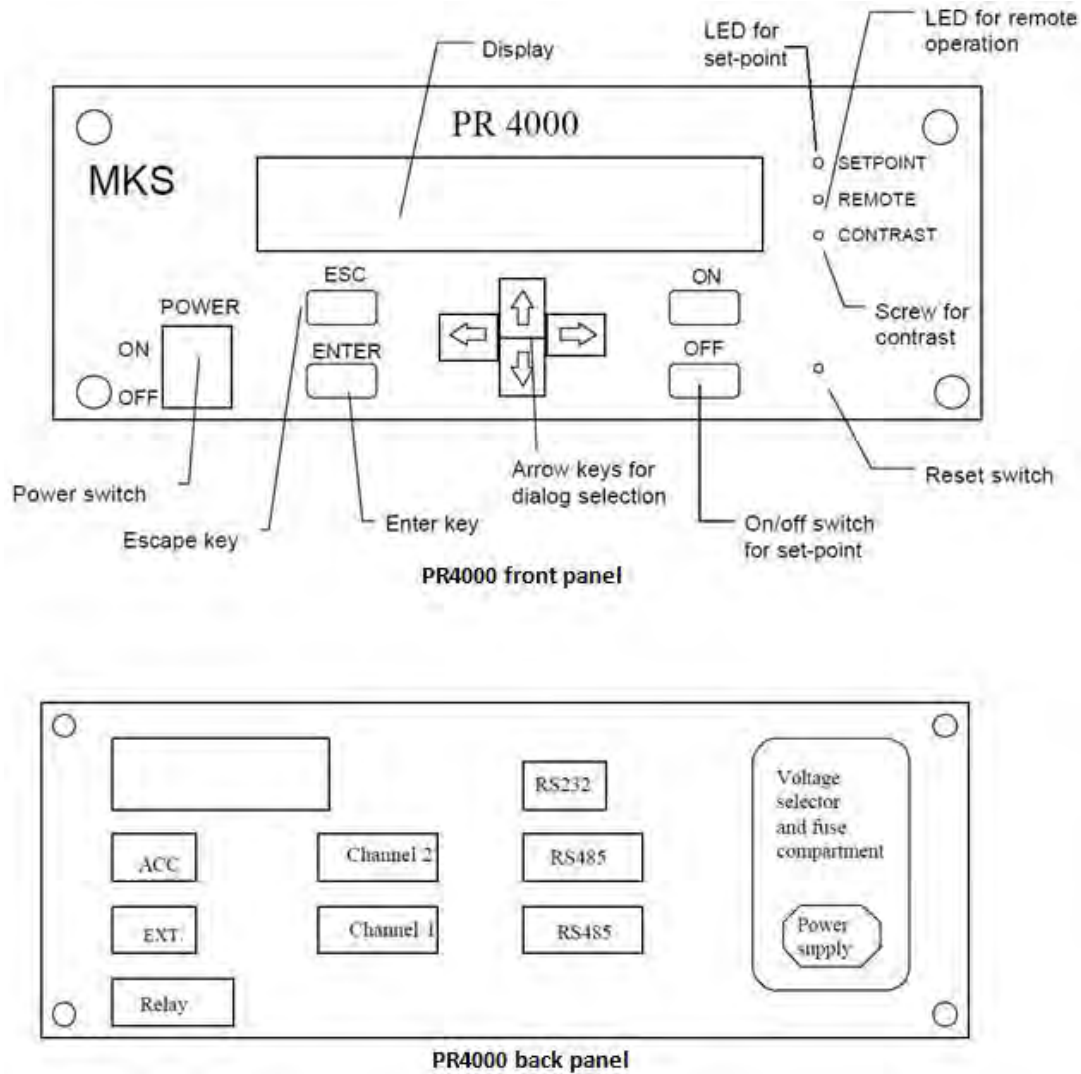


Figure 11. PR4000 Front and Back Panels (After MKS, 2000)¹¹

¹¹ MKS Instruments, *PR 4000 F Instruction Manual* (MKS Instruments, 2000), 13–14.

b. 223B Differential Pressure Transducer

This two-ported transducer measures a bidirectional differential pressure of up to five inches of water with an accuracy of 0.3% of full scale.¹² The sensor is comprised of a metal diaphragm within an Inconel® housing and a ceramic electrode that senses the displacement of the diaphragm. The transducer is powered from the PR4000F unit with a ±15VDC supply and outputs a ±5VDC signal that is linearly proportional to pressure. Electrical connections are made to the terminal block on the transducer per Table 2, and the cable is joined to the PR4000F via RS232 connector.

Cable Connections		
Type 223	Cable Wire Color	MKS Readout Connection
+ 15	Green	+ 15
- 15	White	- 15
COMMON	Black (small) (paired with green)	P COM
	Black (small) (paired with red)	S COM
PRESSURE OUT	RED	PRESSURE IN
No Connection	Black (heavy)	CHASSIS

2-Table 2. MKS 223B Wiring Diagram (From MKS, 1999)¹³

c. 750B Absolute Pressure Transducer

The Type 750B pressure transducer is a single ended sensor made of a metal diaphragm within an Inconel® housing. It has a range of 0–15 psia at an accuracy of ±1% of the reading.¹⁴ Electrical connections are made to both the sensor and the PR4000F power supply via RS232 connection.

¹² MKS Instruments, *MKS Baratron Type 223B Pressure Transducer* (MKS Instruments, 1986), 17.

¹³ *Ibid.*, 8.

¹⁴ MKS Instruments, *700 Series Baratron Pressure Transducers* (MKS Instruments, 1999), 3.

4. Inclined Manometer

An inclined manometer calibrated in inches of water with a maximum readability of 0.05 inches of water was used as an independent, mechanical verification of pressures detected by the MKS Baratron and Scanivalve DSA 3217 pressure transducers.

5. Hot Wire Anemometry (HWA/CTA) System

A Dantec Constant Temperature Anemometer (CTA) system comprised of three 56C01 CTA modules, three 56C17 CTA bridges, filter unit, and one 56N22 mean value module contained within a common housing, was used for instantaneous velocity and turbulence measurements. The system has been configured for the hardware currently used in the wind tunnel experiments. There are four internal, binary switches on the CTA bridge that must be set with the card removed (Figure 12). The indications on the card are such that a white dot on top of the switch is logic 1 and a white dot on the bottom is logic 0.¹⁵

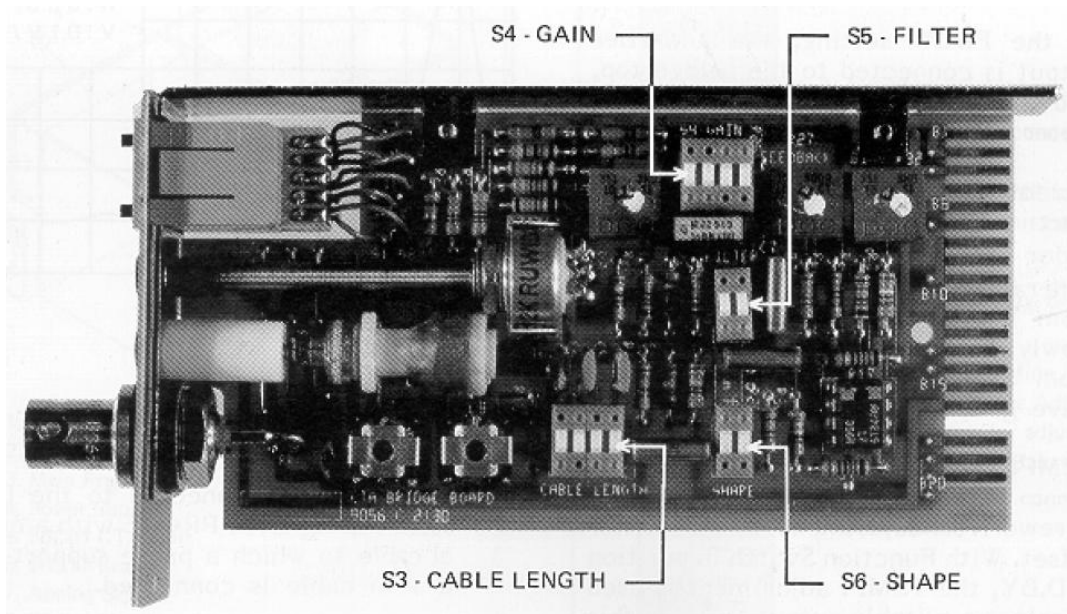


Figure 12. CTA Bridge Internal Switches (From Dantec, 2003)¹⁶

¹⁵ DANTEC Dynamics, *56C17 Manual* (DANTEC Documentation Department, 2003), 5–6.

¹⁶ *Ibid.*, 6.

a. Cable Length, S3

The length of the BNC cable connecting the CTA bridge to the hotwire probe mount is selected via switch S3, with cable length options of 5, 20, and 100m as optional values. The logic value 1000 was entered on this switch to designate the use of a 5m cable.

b. Gain, S4

The switch, S4, controls the gain setting for the servo amplifier on the CTA bridge. This gain was set to the minimum values of 166 and 3477 for AC and DC amplifier gains, respectively, using the logic value of 0000 as directed by the calibration procedure when the optimal setting of the servo amplifier is unknown.

c. Filter, S5

The switch, S5, controls the upper frequency limit of the servo amplifier. The optimal setting for the filter was unknown, causing S5 to be set to the calibration directed setting of 25 kHz using a logic value of 11.¹⁷ This is the lowest bandwidth setting for the CTA bridge filter.

d. Shape, S6

The shape switch, S6, allows the operator to define the shape of the sensor attached to the CTA bridge: flat, fiber/film, or wire. The position of this switch sets the amplifier frequency response of the CTA bridge to obtain the best possible bridge balancing during calibration.¹⁸ All experiments conducted with CTA used hot wires as a sensor with S6 (the feedback system response) set for the wire setting with the logic value of 11.

¹⁷ Ibid., 7.

¹⁸ Ibid., 7.

E. VELMEX BISLIDE TRAVERSING ASSEMBLY

1. BiSlide Unit

The traverse assembly for navigating equipment in the test section is a model MN10–0300-M02–30 slide manufactured by Velmex, Inc. (Figure 13). The mechanism is an electric motor driven, screw drive with a 30 inch design travel. The lead screw has a 2.0 mm advance/turn which results in 0.005 mm/motor step (0.0002 inches/step). The lead screw nut or StabilNut is adjustable, controlling a tension plate which has been set to minimize the amount of backlash when stopping the drive motor. Two repositionable limit switches are included on the BiSlide to set the boundaries for carriage travel and reduce the risk of damage to equipment moving with the test section.

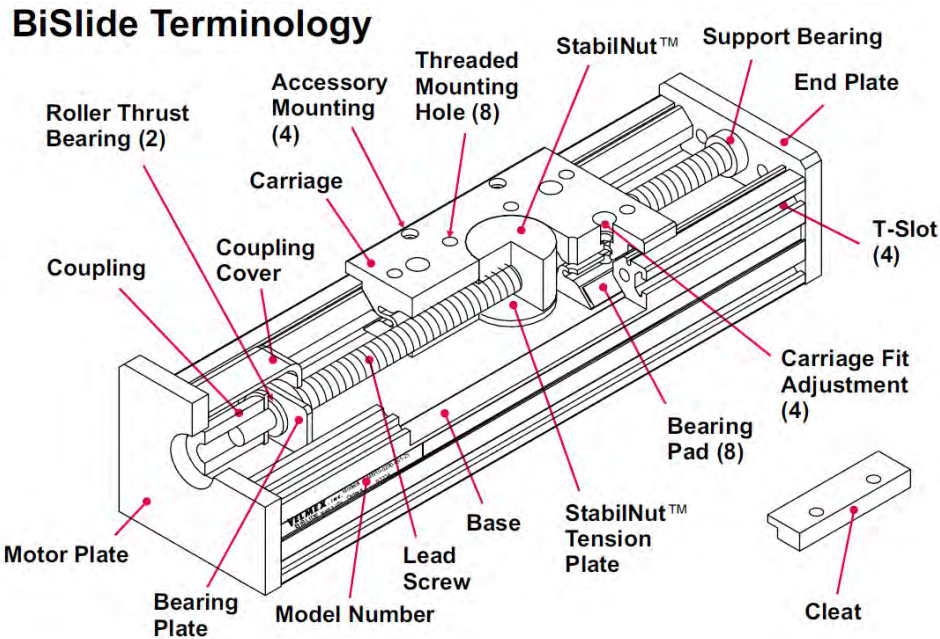


Figure 13. BiSlide Traverse Assembly (From Velmex, 2011)¹⁹

2. Traverse Motor

The traverse motor for the BiSlide is a NEMA Type 34D, Slo-Syn® stepper motor, allowing the operator to position items in the test section in discrete increments. The motor rotates at 200 RPM and has a backlash protection system to minimize starting

¹⁹ Velmex, Inc., http://www.velmex.com/bislide/motor_bislide.html, accessed 6 September 2011.

and stopping effects on positioning. The motor is rated for 2.5 VDC, 4.6 Amp. supply, continuous operation to provide delicate positioning of the BiSlide assembly within a noncumulative $\pm 3\%$ of a step (1.5×10^{-4} mm) with one step equaling 1.8° of rotation, or 0.9° when half-stepping techniques are utilized. The position within the test section must be verified before each use by positioning the probe mounting arm at the upper or lower limit switch (top or bottom wall of the test section) and moving to the vertical centerline by instructing the stepper motor to move 45,700 steps in the appropriate direction, thus ensuring testing is occurring in the actual centerline of the test section.

3. VP9000 Stepper Motor Controller

The VP9000 controller has the capacity to control four stepper motors and their associated limit switches either automatically through communication with the PC via RS-232 cabling, or through a hand-held, corded remote control with push button inputs (Figure 14). The VP9000 has a digital display that shows the motor position in number of steps both at rest and during traversal. The VP9000 must be programmed via the front panel for the particular traverse motor; any changes in the traverse motor without verifying the VP9000 settings may result in damage to the traverse motor.



Figure 14. VP9000 Stepper Motor Controller

F. DATA ACQUISITION AND PROCESSING PACKETS

Three distinct programming packages were integrated in order to allow the various instrumentation and data acquisition equipment to communicate with each other and the host PC. Appropriate code was developed in LabVIEW, DAPL, and DSALink3 for the wind tunnel, as well as the use of both Microsoft Excel and MATLAB for data gathering, processing, and graphics handling.

1. DSALink3

A modified form of the Scanivalve proprietary software suite, DSALink3, Version 3.03 is installed on the wind tunnel PC. The software is a 32-bit application designed for operation with Windows XP or Windows 2000 and assistance from Scanivalve was required to modify the software in order to operate it with the 32-bit Windows 7 operating system present on the host PC. DSALink3 enables the user to setup a new connection, employ preprogrammed control functions on the DSA 3217, and communicate with the PC via Ethernet cabling.

2. Data Acquisition Programming Language, DAPL 2000

The Microstar system circuit boards communicate via DAPL 2000 with the high-level controlling program on the PC running in LabVIEW. DAPL's scripts handle the interfaces between the DAP and attached sensors, performs configuration management to ensure compatibility and ensure platform independence, and executes all data transfer functions (Figure 15). DAPL tasks communicate through buffering structures called pipes. The PC and/or sensors transmit and download data from pipes where it is held temporarily until the next sequential task is ready. DAPL keeps the data in correct sequence utilizing a first-in, first-out (FIFO) basis. During processing, data samples are recorded, output signals are used, and the temporary intermediate values are discarded. All of these activities require intermediate memory buffers. The DAPL system handles

all task synchronization and memory buffer management. (**Note:** there is a DAPL 3000 suite which works with USB communication and is not compatible with the PCI interface DAP boards.)²⁰

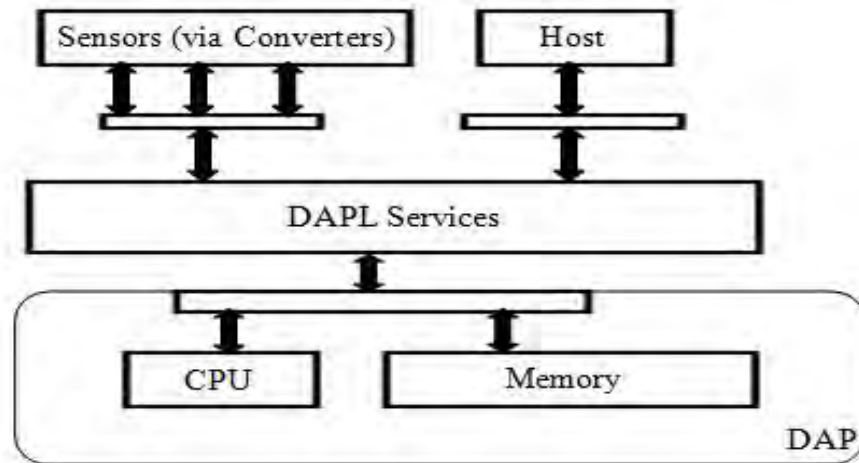


Figure 15. DAPL Architecture (After Microstar, 2011)²¹

3. LabVIEW

LabVIEW is a graphical programming language (trademarked by National Instruments) that is compatible with a wide range of software and hardware applications and contains a vast library of prefabricated functions for integration into user developed virtual instruments (VIs). Thus, it is compatible with a large number of NI data acquisition and third-party devices, allowing the wide range of equipment being employed in these tests to collect, transmit, and analyze the raw data collected from experiments.²² (**Note:** the LabVIEW codes are written for the current configuration of LabVIEW. Altering the version of LabVIEW or installing updates to LabVIEW software may render current VIs inoperable.)

²⁰ Microstar Laboratories, Inc., http://www.mstarlabs.com/software/dapl/tabs.html#_overview, accessed 7 September 2011.

²¹ Ibid.

²² National Instruments, <http://www.ni.com/labview/applications/daq>, accessed 16 August 2011.

a. DSA 3217

The DSA 3217 pressure sensor code required the marriage of LabVIEW and the DSALink3 software to ensure the correct Internet protocol addressing and link layer communication between the PC and the sensor. The DSALink3 forms the line of communication between the PC network address (191.30.80.92) and the DSA 3217 address (191.30.80.91). LabVIEW uses this established link to execute the ‘read’ instruction to the DSA 3217 for data acquisition. This VI automatically prompts the user to save the data from the 16 pressure ports to a user defined file location. The user may opt to create a new file for each iteration or append the data to an existing file by selecting the appropriate push button on the front panel of the VI. Data is saved as a 1x16 row vector, but may be changed by selecting the ‘Transpose’ button on the front panel (Figure 16). The user may also change the number of significant digits for the saved data by altering the format box located at the bottom of the front panel; Figure 13 shows the front panel for the VI configured to append a file with the data saved as a column vector with six significant digits on each value. All operations for this VI are conducted through the front panel.

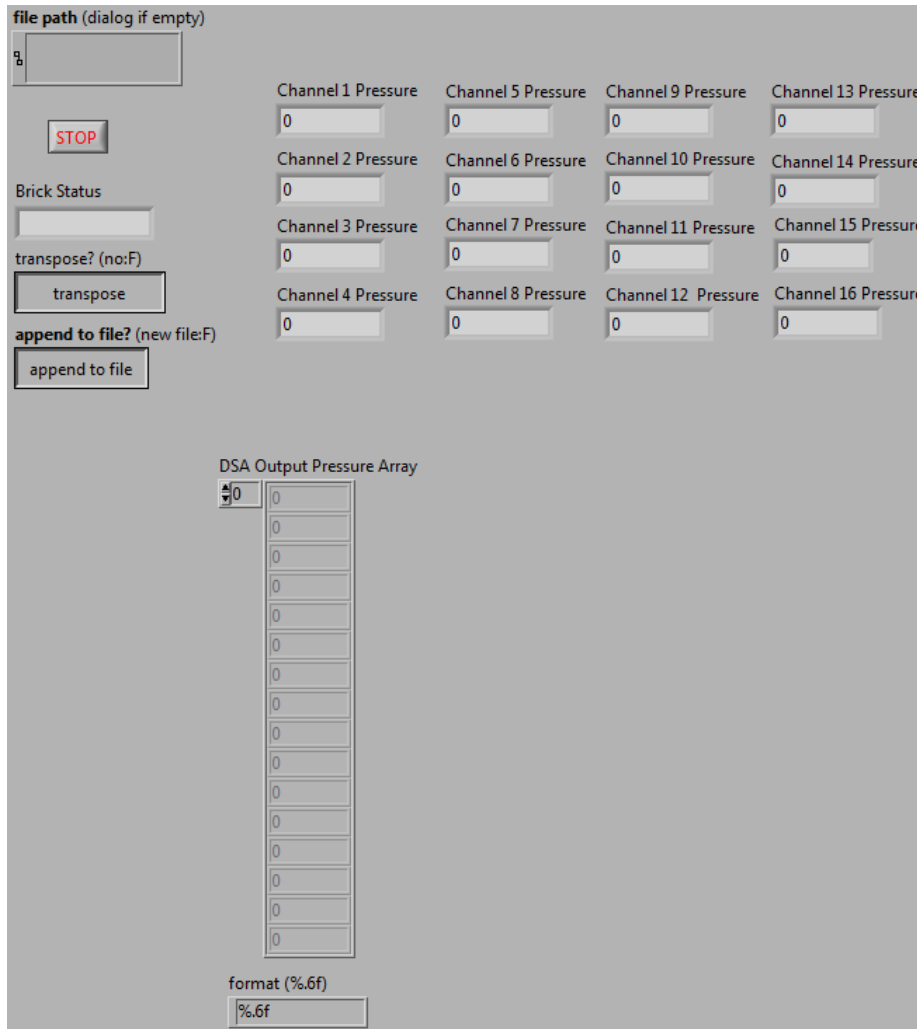


Figure 16. DSA 3217 LabVIEW Front Panel

b. Data Acquisition Processor

A LabVIEW VI, named *dapdaq.vi*, for collecting and processing analog and digital signals from the MSXB 048 and MSXB 038 was modified for use with the Halligan wind tunnel equipment from an existing suite developed for NPS and used at NASA’s Ames Research Center (Figure 17). The DAP code allows the user to select any combination of up to two digital channels and 16 analog channels, vary the sampling frequency as necessary for the monitored signal, and choose the number of total sample

points to be collected in the sample set. All operations for this VI and associated sub-Vis are controlled from the front panel (Figure 18); no control functions are required within the VI code.

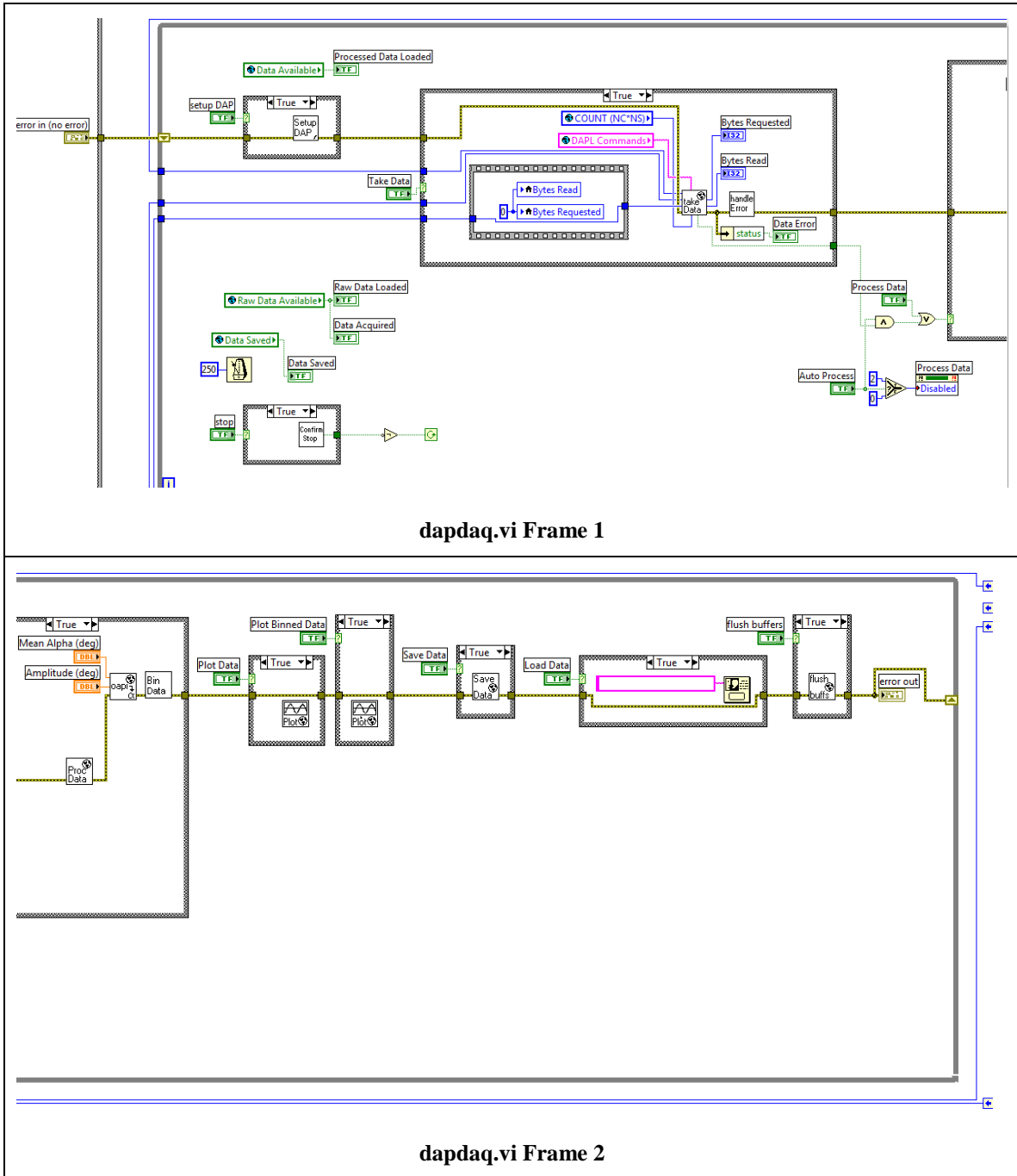


Figure 17. DAP LabVIEW Code

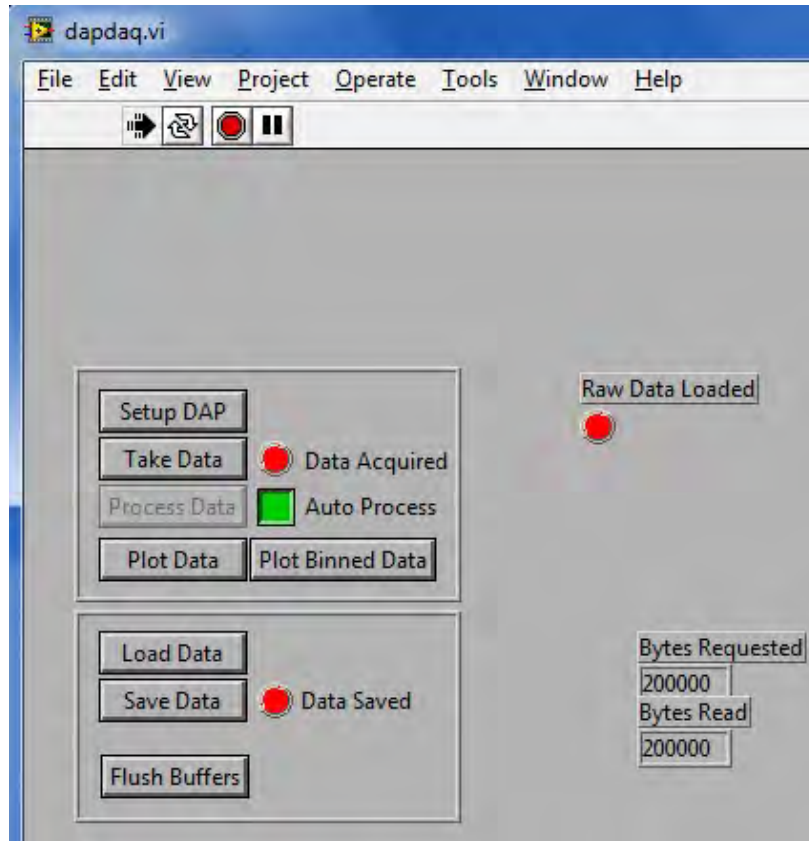


Figure 18. DAP LabVIEW Front Panel

c. Velmex BiSlide

LabVIEW code (Figure 19) for the BiSlide assembly was developed to allow automatic positioning of the traversing mechanism for precision placement of sensors in the test section. The current configuration of the code provides the ability to move the motor by an integer number of steps, move to a defined location (a position on the slide described by a number of steps from the endpoint of the lead screw), or move to the home location, identified as the test section centerline for this application. The pink outlined box with 'I1, M70000, R' is the user's means to input commands to the motor via LabVIEW, with this example instructing motor #1 to move 70,000 steps in the positive (downward) direction. The R is a carriage return for the Velmex controller and is interpreted as an end of command; it must be received for the Velmex controller to

send a signal to reposition the traverse motor. The user controls this VI by typing the desired command into the input box in the code; there is not a front panel interface for input.

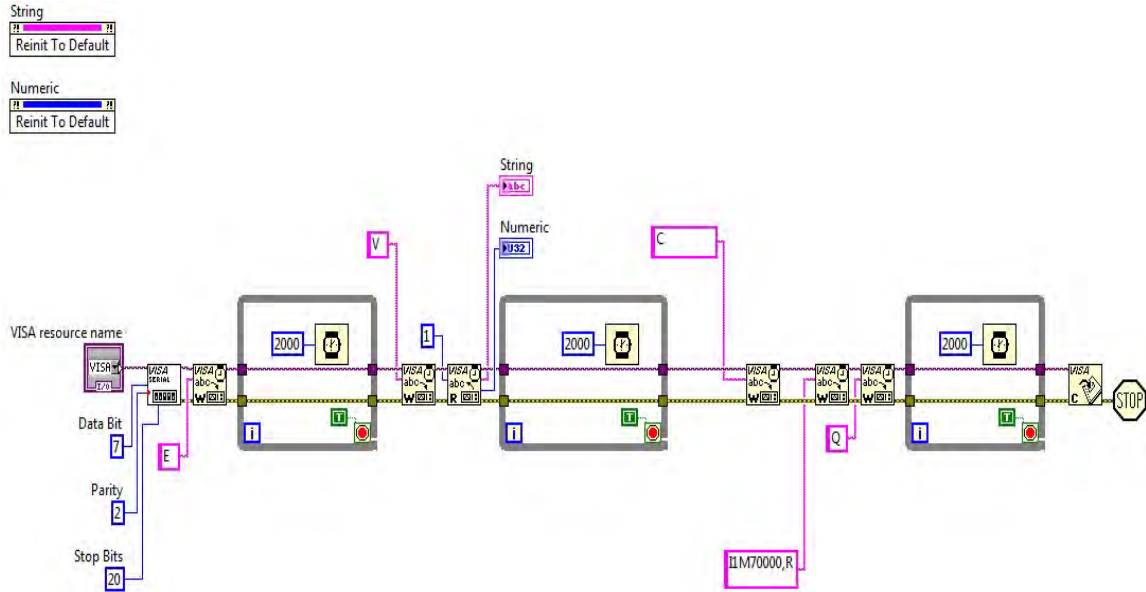


Figure 19. BiSlide LabVIEW Code

4. MATLAB

A MATLAB function was developed to calculate and plot the turbulent velocity fluctuations power spectrum from CTA data using Hanning window filtering to reduce the production of side lobes when the signal is transformed from the time to the frequency domain using the standard FFT techniques.²³ The code is customizable by the user with variables such as sampling frequency, Hanning window length, and number of samples to be analyzed as user controlled variables for the analysis (Figure 20). The signal must be saved in a text file for the function to read the data into MATLAB, with the inputs to the function being the filename location for the signal (dir), window length (L), and the sampling frequency (Fs). Increased resolution is obtained by adding the appropriate number of zeroes to the data set.

²³ Thomas Krauss, Loren Shure, and John Little, *Signal Processing Toolbox for Use with MATLAB* (The MathWorks, Inc., 1993), 2.169–2.172.

```

function [Px, f] = PSPECTRA(dir, L, Fs)
%PSPECTRA conducts a fft of an input signal (fx) and plots
%the RMS Power vs. frequency on a log-log graph.
%   where Fs is the sampling frequency in Hertz and L is the
%   length of the Hanning window function.
fx=load('dir');
wl=hanning(L);
[Px,f]=psd(fx,L,Fs,wl,0,'none');
loglog(f,Px*norm(wl)^2/sum(wl)^2,'k'); %% plot on log-log scale
ylabel('RMS Power/Frequency (V^2)')
xlabel('Frequency (Hz)')
title('Power Spectrum')

end

```

Figure 20. MATLAB Power Spectrum Code

III. EXPERIMENTAL PROCEDURES AND RESULTS

Current software and hardware configuration provides four general testing capabilities: 2-D velocity determination across the center of the test section utilizing the pressure rake, wall static pressure distribution mapping, boundary layer probe or CTA traversal along the vertical axis, and examination of flow phenomena with a flat plate inserted within the test section. Each test requires a different physical setup and executes a different combination of LabVIEW VIs and Microsoft Excel templates for data acquisition and processing.

A. WIND TUNNEL CALIBRATION

1. Test Setup

a. Pitot-Static Tube

(1) Insert the pitot-static tube (Figure 6) in the Position 0 wall static pressure port of the test section and connect it to ports 1 and 2 of the DSA 3217 for tunnel speed determination versus the speed dial setting.

(2) Verify the pitot-static tube is properly oriented in the wind stream with the stagnation pressure port facing directly toward the test section inlet.

(3) Ensure the DSA 3217 is energized for a minimum of one hour prior to data collection for proper warm up and stabilization.

b. DSA 3217 Connection

(1) Start and login to the PC. Open the *Velocity.xlsx* template on the PC's desktop and save it as a separate file with the date as the file name, e.g. *17AUG11.xlsx*. Obtain weather data from <http://weather.noaa.gov/weather/current/KMRY.html> and record the information in the template.

(2) Unplug the Ethernet cable from the wall connection and plug it into Port 1 of the router located on top of the instrument cabinet. Start the Windows Network and Sharing Center and click on the Local Area Connection link (Figure 21).

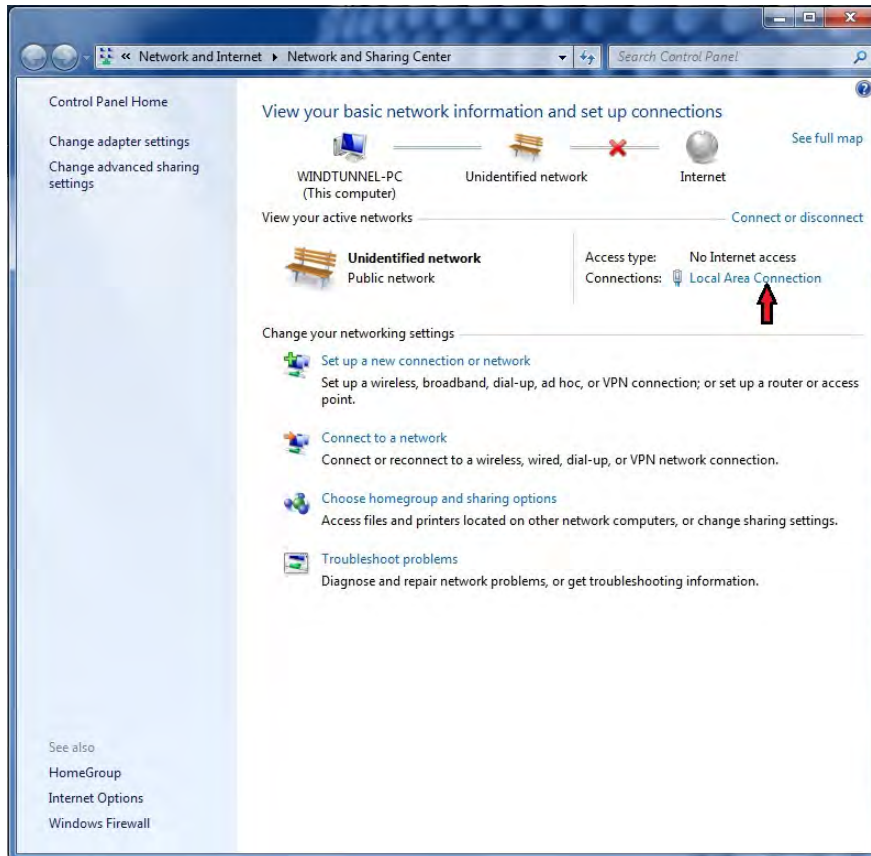


Figure 21. Connecting to DSA 3217

(3) In the popup window that appears, click on the ‘Properties’ button, double click on ‘Internet Protocol version 4 (TCP/IPv4)’ in the window, and click on ‘Properties.’

(4) In the newest popup window, click on ‘Use the following IP address’ and enter ‘191.30.80.92’ in the address block, press tab and ensure the Subnet mask 255.255.0.0 appears beneath the entered IP address (Figure 22).

(5) Press the buttons ‘OK,’ ‘OK,’ and ‘Close,’ and exit the Windows Network and Sharing Center.

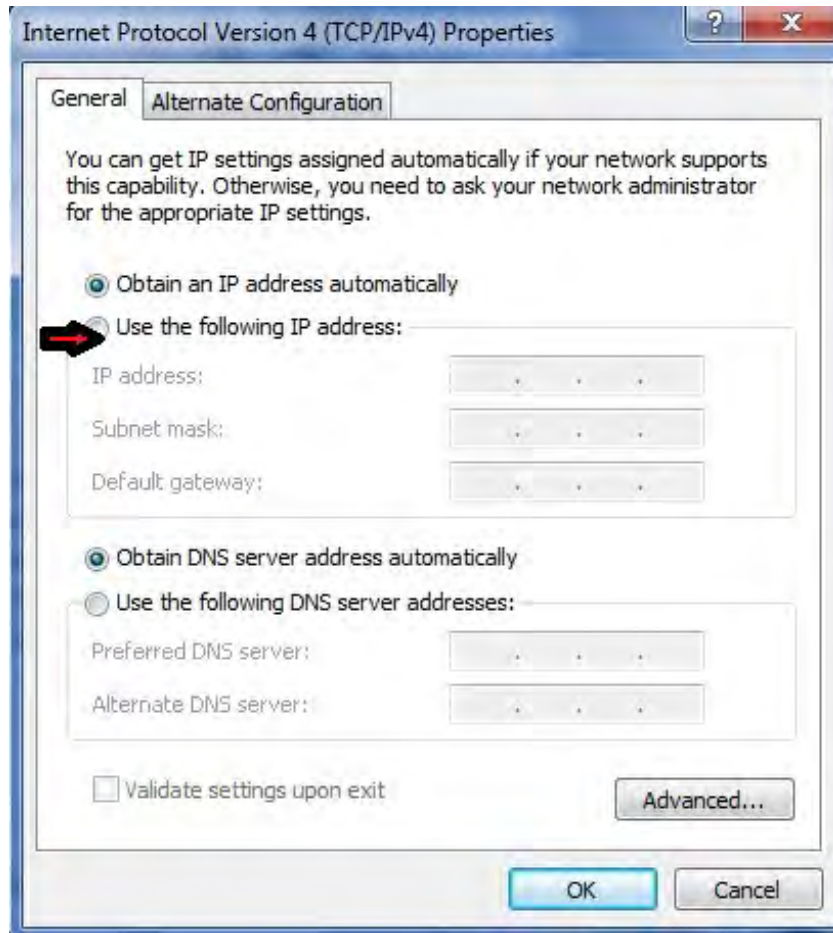


Figure 22. Internet Address Entry for DSA 3217

c. Wind Tunnel Warm Up

(1) Check the main power supply breaker on the bottom of the back panel of the control unit is on (horizontal position).

(2) Ensure the speed dial on the wind tunnel control panel is set to zero (fully counterclockwise) and the tape over the vent opening at the back end of the test section is covering the opening and in good repair.

(3) Depress the green ‘Mains Supply’ on button and observe the green light illuminate on the wind tunnel controller. Depress the green ‘Fan’ run button and observe the green light illuminate (Figure 23).



Figure 23. Wind Tunnel Control Panel

(4) Rotate the speed dial clockwise fully; the dial indicator will roll over and indicate approximately 000–001. Allow the wind tunnel to operate at full speed for one hour for temperature stabilization prior to experimental data collection (Figure 23).

(5) Once the warm up has concluded, rotate the speed dial fully counterclockwise to a setting of 000 and secure the fan by depressing the ‘Fan’ red stop button and observing the green run light extinguish.

d. DSA 3217 CalZero

(1) Start DsaLink3 by double clicking the desktop icon.

(2) Under ‘Open Existing DSA Connection,’ click on the IP address ‘191.30.80.91’ and ensure the address appears in the ‘Open new Dsa Connection’ box. Press ‘Connect’ (Figure 24); connection requires approximately 2 seconds.



Figure 24. Connecting to DSA 3217

(3) Ensure 'Connected to 191.30.80.91 (Model 3217)' and 'Dsa status: READY' appear in the bottom of the window (Figure 25).

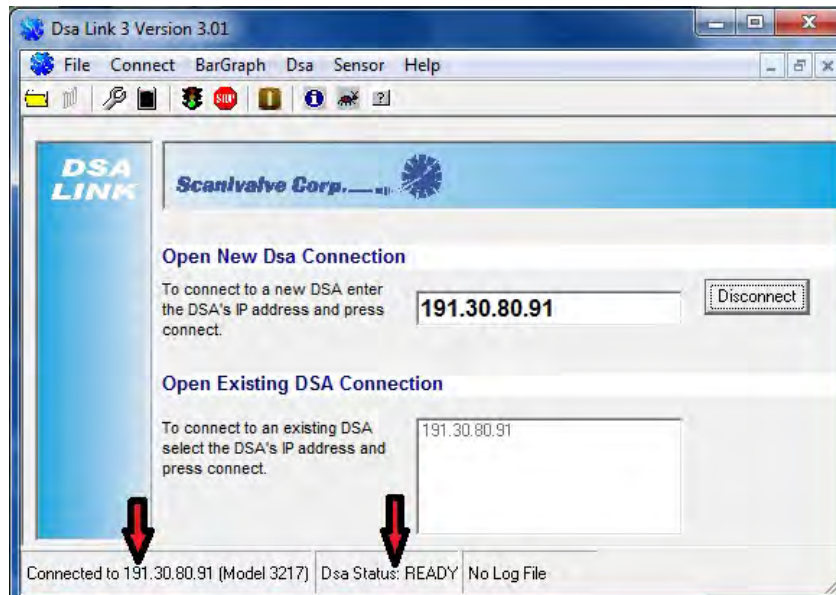


Figure 25. Verifying DSALink Connection

(4) In the DsaLink3 menu, select the Dsa tab and Cal Zero. Ensure the Dsa Status changes from 'READY' to 'CALZ' (Figure 26) and returns to

‘READY’ (Figure 25). A clicking noise will be made by the DSA 3217 as it cycles its reference pressure port solenoid valve to equalize with atmospheric pressure.

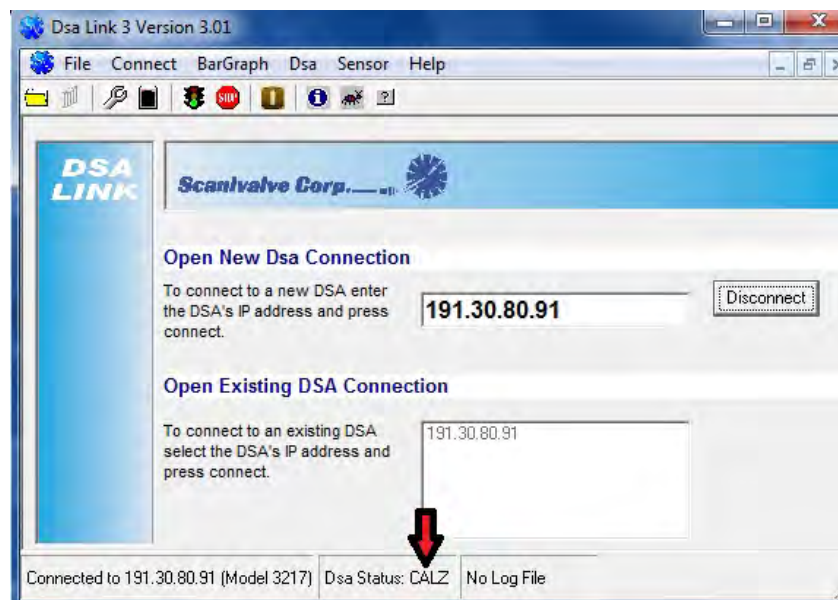


Figure 26. DSALink CalZero Response

(5) Press ‘Disconnect’ and verify the link is terminated by observing ‘No connection’ in the lower left hand corner of the window. Exit DsaLink3.

e. DSA 3217 VI Setup

(1) On the PC desktop, start LabVIEW and open the *PressureBrick.vi* file (also present as a shortcut on the PC desktop).

(2) Set the desired number of significant digits (default is three) by changing the %3f variable. The user may also set the VI to record data in a different file with each execution or to append an existing file with each event by depressing the appropriate push button on the front panel of the VI (Figure 14).

(3) Depress the run arrow on the front panel of the DSA 3217 VI to record rest pressures from the static and dynamic pressure connections of the pitot-static tube.

f. Establish Initial Conditions

(3) Depress the green 'Fan' start button, note the green run light illuminate, and Turn the speed dial clockwise until the desired tunnel speed is set.

(3) Verify the *PressureBrick.vi* and Excel spreadsheet are open and weather data has been entered with the spreadsheet saved with the current date as the filename.

(3) Allow the wind tunnel to run for a minimum of five minutes prior to the collection of each data point to ensure steady state conditions have been established due to the small sensing port size and tubing connection to the PST.

2. Conduct of Testing

a. Data Collection

(1) Set the wind tunnel speed dial to 300.

(2) Observe the five minute stabilization time, then depress the run arrow on the front panel of the VI to collect the static and stagnation pressure data. Enter the file name in the pop-up dialogue box to which LabVIEW will write the data and press 'Enter.'

(3) Turn the speed dial clockwise by increments of 50 and repeat steps III.A.2.a.(2)-(3) for data collection until the data is acquired at the maximum setting of 1000.

b. Securing the Wind Tunnel

(1) Rotate the speed dial fully counterclockwise until the indicator shows 000.

(2) Depress the red stop button labeled 'Fan' and the red 'Mains Supply' off button and ensure the green indicator lights for both functions extinguish.

3. Tunnel Speed Calculation

a. Data Transfer

Transfer the pressure data from Ports 1 and 2 of the DSA 3217 from the file LabVIEW created to the Excel file, ensuring the pitot-static tube (PST) stagnation (P_o) and static pressures (p) are in the correct columns in the Excel file (Figure 27).

	A	B	C	D	E	F	G	H	I	J	K
1	Temp:	55°F									
2	PATM:	29.91" Hg									
3	RH:	63%									
4											
5			Dial Setting	0	150	200	250	300	350	400	450
6			PST-P0 (psi)	-0.000481	0.003183	0.004726	0.005305	0.005498	0.006462	0.010031	0.0136
7			PST-p (psi)	0	-0.001052	-0.001722	-0.002488	-0.003731	-0.005262	-0.007176	-0.009185
8											
9			Wind Speed (m/s)	0.00	6.90	8.52	9.37	10.19	11.49	13.91	16.01

Figure 27. Velocity Template (example)

b. Determining Tunnel Speed

The tunnel speed is automatically calculated in meters per second (m/s) assuming the compressible, isentropic flow in the test section (Equation 1). The speed of sound in air and the atmospheric pressure are assumed to be constant over the small range of temperatures and pressures experienced by the wind tunnel ($\pm 20^\circ\text{F}$ and $\pm 0.2''$ Hg, respectively). The use of Equation 1 allows the calculation of all wind speeds within the test section, including accelerating flow around any models tested in the wind tunnel, thus minimizing the number of equations required for testing.

$$U_\infty = a_o \sqrt{5 \left\{ \left[\frac{(P_1 - P_2)}{P_o} + 1 \right]^{2/7} - 1 \right\}}$$

Equation 1 Tunnel speed Calculation²⁴

Where,

a_o is the speed of sound at sea level; 340.294 m/s,

P_o is the static air pressure at sea level; 14.696 psi,

$P_1 = \text{PST-P}_o$,

$P_2 = \text{PST-p}$, and

U_∞ is the tunnel speed in m/s

²⁴ NASA, <http://www.grc.nasa.gov/WWW/k-12/airplane/isentrop.html>, accessed 19 September 2011.

4. Calibration Results

a. Problems and Resolutions

During the conduct of calibration testing, it was noted that the differential pressures from the pitot-static tube were drastically different between the MKS Baratron and Scanivalve DSA 3217 sensors with the MKS averaging only 15% of the DSA 3217 detected pressure (Figure 28).

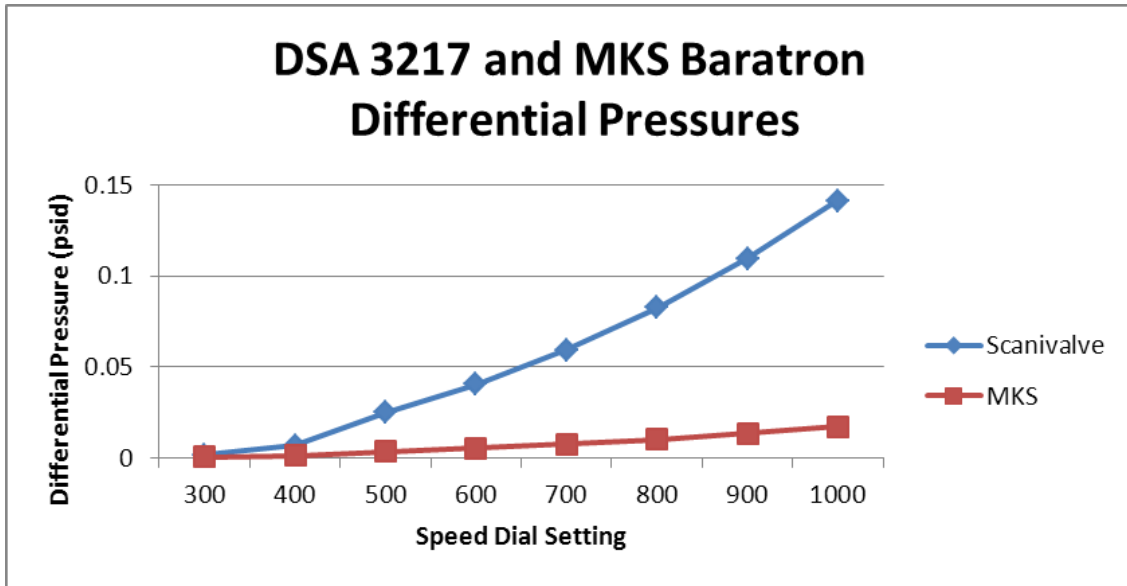


Figure 28. MKS Baratron and DSA 3217 Indicated Pressure Differences

With the MKS pressure suspect, the pitot-static tube with the Scanivalve DSA 3217 transducer was connected in parallel to an inclined manometer with the contraction cone pressure sensing ports of the wind tunnel connected to Ports 3 and 4 of the DSA 3217, and the same calibration procedure was re-performed. The tunnel speeds calculated from the manometer differential pressure averaged within one percent of the DSA 3217 over the full speed range of the wind tunnel, with a maximum difference of 1.6% at a speed dial setting of 300. The tunnel speed calculated from the contraction cone pressure ports averaged 18% lower than the DSA 3217, and the maximum difference was 27% lower at a speed dial setting of 500 (Figure 29). With the Scanivalve DSA 3217 verified to be indicating the true pressures, the MKS Baratron transducers and inclined manometer were disconnected and the PR4000F control unit disconnected from the PC.

Wind Speed Comparison by Sensor

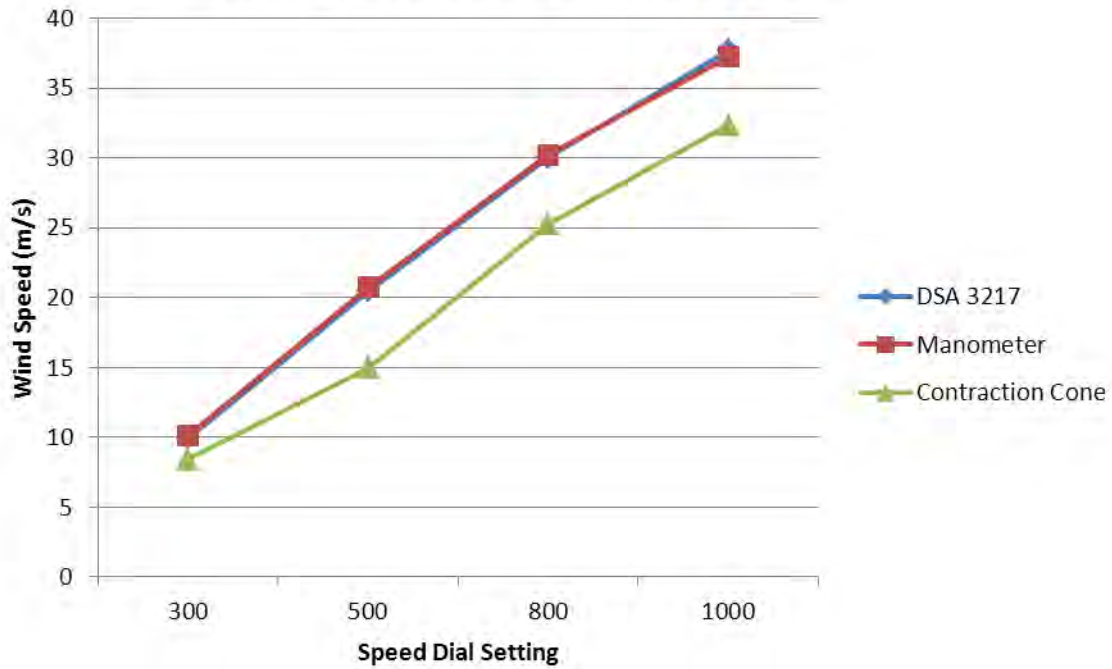


Figure 29. Tunnel Speed Comparison by Sensor Type

b. Tunnel Speed Results

The calibration of the wind tunnel revealed that the tunnel speed calculated from the pitot-static tube inserted at Position 0 ranged from 0–38 m/s (Figure 30). The tunnel speed varied by $\pm 1\%$ maximum based on test data collected five minutes apart for 30 minutes at speed dial settings of 400, 600, 800 and 1000. The discontinuity demonstrated at a speed dial setting between 300 and 500 appears to be a characteristic of this wind tunnel and cannot be easily explained. The change in slope shown in Figure 30 is typical of all test runs conducted on the MAE wind tunnel.

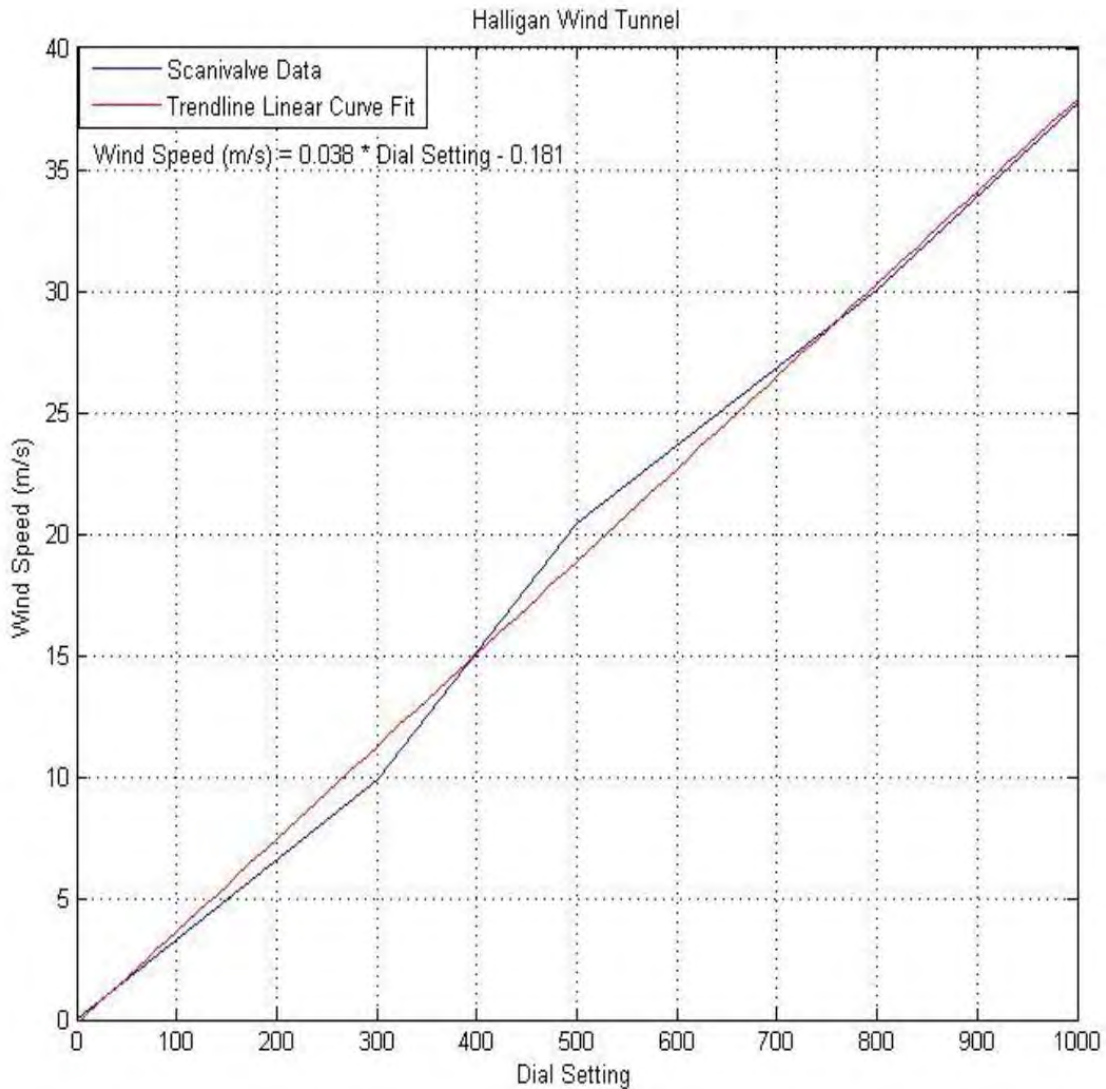


Figure 30. Test Section Tunnel Speed vs. Speed Dial Position

B. 2-D VELOCITY MAPPING

1. Test Setup

a. Pressure Rake installation

- (1) Perform or verify Step III.A.1.a is completed.
- (2) Connect one 0.063" tube between the Position 4 static pressure connection and port 3 of the DSA 3217.

(3) Remove the plastic plugs from the Perspex test section windows and install the nylon bushings into the openings.

(4) Remove the operator side window.

(3) Install the pressure rake in the test section by inserting the ½” threaded lead screw through the bushing on the far side window and resting the rake on the bottom of the test section.

(4) Remove the Position 5 static pressure port fixture. With the lead screw through the far side window, thread the thirteen 0.063” tubing through the Position 5 static pressure port and attach them to the desired pressure rake sensors. The tubing is labeled on both the rake and DSA 3217 ends with numbers from 21 through 34 for tracking purposes.

(5) Once the tubing is attached, reinstall the near side window by sliding the bushing installed in the window over the lead screw and aligning the four bolt holes with the studs on the wind tunnel.

b. Instrument Setup and Tunnel Warmup

Conduct Steps III.A.1.b-f, with one exception: open the Excel template named *2DVel.xlsx* and save it with the same naming convention described previously.

2. Conduct of Testing

a. Data Collection

(1) Set the wind tunnel speed dial to the desired speed.

(2) Observe the prescribed five minute stabilization time, then depress the run arrow on the front panel of the VI to collect the pressure data from the pressure rake, static pressure port, and pitot-static tube. Enter the file name in the pop-up dialogue box to which LabVIEW will write the data and press ‘Enter.’

(3) Traverse the pressure rake manually by the desired distance and observe the five minute stabilization time.

(4) Perform Steps III.B.2.a.(2)-(3) until the required data sampling points have been recorded.

b. Securing the Wind Tunnel

(1) Rotate the speed dial fully counterclockwise until the indicator shows 000.

(2) Depress the red stop button labeled ‘Fan’ and the red ‘Mains Supply’ off button and ensure the green indicator lights for both functions extinguish.

c. Data Processing

(1) Transfer the data from the LabVIEW created file to the *2DVel.xlsx* template by copying and pasting. Ensure the data matrix aligns with the appropriate rows and columns in the template (Figure 31).

Temp: 71°F											
PATM: 29.98" Hg											
RH: 55%		Horizontal and Vertical position in inches									
Dial Setting: 1000		Vert.	Horiz	66.67%	55.56%	44.44%	33.33%	22.22%	11.11%	0.00%	
Channel	Nomenclature	z (@CL z=0)	y (@CL y=0)	+6	+5	+4	+3	+2	+1	0	
1	PST-Po	N/A	N/A	0.087419	0.087516	0.086937	0.088963	0.089253	0.090025	0.089446	
2	PST-p	N/A	N/A	-0.042475	-0.044293	-0.044675	-0.045249	-0.045823	-0.046302	-0.047162	
3	1" (from top)	+8	88.89%	0.104908	0.104422	0.10413	0.104616	0.104811	0.105491	0.106561	
4	2" (from top)	+7	77.78%	0.104849	0.104562	0.104084	0.104371	0.104658	0.105327	0.106475	
5	4" (from top)	+5	55.56%	0.104888	0.104614	0.103883	0.104248	0.104888	0.105346	0.106352	
6	6" (from top)	+3	33.33%	0.104648	0.104282	0.103642	0.104191	0.104831	0.105014	0.10602	
7	7" (from top)	+2	22.22%	0.104877	0.104417	0.10405	0.104693	0.104968	0.105152	0.106254	
8	8" (from top)	+1	11.11%	0.104462	0.104289	0.103944	0.104548	0.104548	0.104979	0.106187	
9	9" (from top)	0	0.00%	0.104509	0.104407	0.103896	0.104611	0.104815	0.105326	0.106245	
10	10" (from top)	-1	-11.11%	0.104751	0.104648	0.104033	0.104853	0.104956	0.105366	0.086711	
11	11" (from top)	-2	-22.22%	0.105152	0.104733	0.104104	0.104628	0.105257	0.105676	0.086596	
12	12" (from top)	-3	-33.33%	0.105149	0.105046	0.104426	0.105253	0.105253	0.105976	0.086041	
13	14" (from top)	-5	-55.56%	0.105192	0.105821	0.104772	0.105192	0.105612	0.106345	0.106975	
14	16" (from top)	-7	-77.78%	0.105119	0.10612	0.105119	0.105319	0.105519	0.10642	0.106821	
15	17" (from top)	-8	-88.89%	0.105656	0.105362	0.104674	0.105558	0.105755	0.106344	0.106934	
16	P wall static (Pos 4)	N/A	N/A	-0.097315	-0.099235	-0.098224	-0.093475	-0.08347	-0.064877	-0.059723	
Windspeed (pitotstatic) (m/s)				38.1783493	38.4578586	38.4292	38.8057113	38.9300125	39.1092811	39.149434	

Figure 31. 2-D Velocity Template (example)

(2) Tunnel speeds are automatically determined as in Step III.A.3.b for both the pitot-static tube and the pressure rake. Pressure rake speed calculations are based on the Position 4 wall static pressure for that iteration. Plots for both the pitot-static and the 2-D tunnel speeds are generated automatically.

3. 2-D Mapping Results

The 2-D mapping was conducted at two speed dial settings, 500 and 1000, with the pressure rake inserted through the access ports on the two Perspex windows of the test section. Twelve of the pressure rake tubes were connected to the DSA 3217, as well as the pitot-static tube, and the wall static pressure connection at Position 4 (the port closes to the plane in which the pressure rake sensor tips were located). Positions are documented as a percentage of the 18 inch vertical and horizontal span with zero being centerline of the test section. The average tunnel speed during the conduct of the test was 38.78 m/s by PST, while the average tunnel speed measured by the pressure rake at Position 4 was 46.18 m/s, a difference of 19.1%. The maximum variation of tunnel speeds from the average in the measured plane was from 12.4% below to 3.9% above the average. The minimum tunnel speeds occurred at positions along the spanwise centerline in the lower half of the test section (Figure 32). Incorporating the 0.12% possible pressure measurement error results in a slight improvement to the velocity distribution with the maximum velocity remaining 3.5% above the mean, but the minimum velocity improving slightly to be 10.8% below the average velocity in the plane. It is due to the small pressures (0.11 psi and less) that the small error in measurement can have this effect on the calculated velocities, however, the difference in the mean velocity of the wind tunnel in the measured plane with this error was less than 1%. It is possible that this defect in the velocity profile is due to a low-frequency transient within the wind tunnel which has not succumbed to its steady state values. Examination of this with increased settling time for pressure rake stabilization time or the attachment of a manometer to view pressure changes could aid in determining if this is the case.

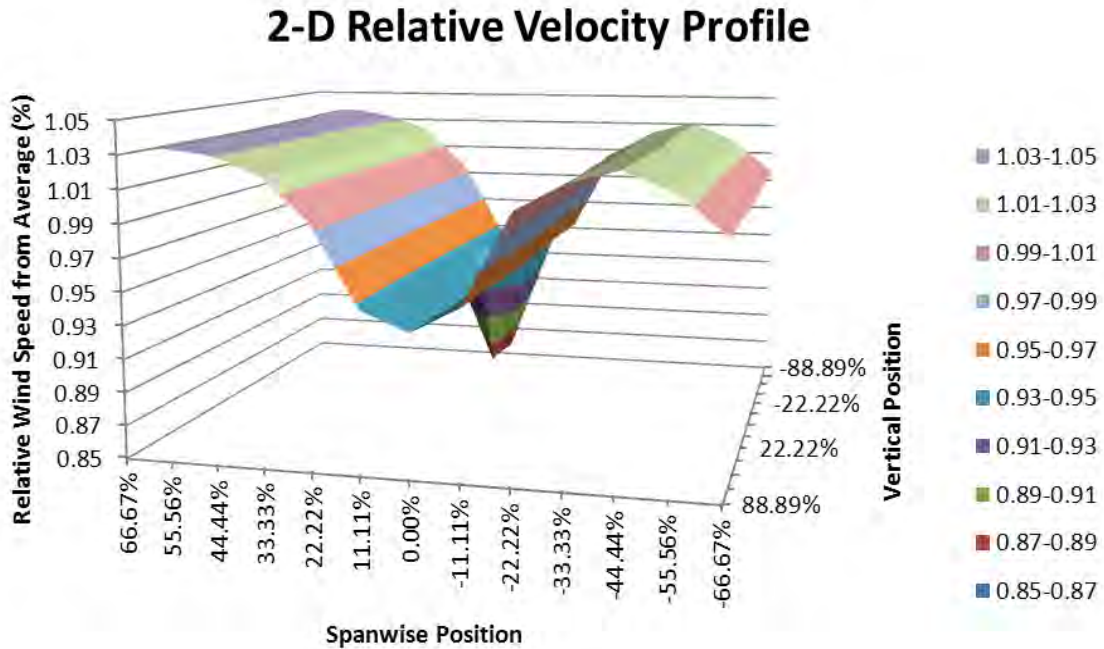


Figure 32. 2-D Relative Velocity Profile

C. WALL STATIC PRESSURE DISTRIBUTION MAPPING

1. Test Setup

a. Tunnel Setup

- (1) Perform or verify Step III.A.1.a is completed.
- (2) Install or verify installed the wall static pressure plugs.
- (3) Connect one 0.063" tube between each of the wall static pressure connections and the sensing ports of the DSA 3217. Ensure the wall static position vs. DSA 3217 port is recorded for tracking purposes.
- (4) Remove the operator side window and verify the bottoms of the plastic plugs are flush with the top of the test section. Reposition them as necessary by tapping in or out to make the surfaces as flat as possible.
- (5) Reinstall the operator side window.

b. Instrument Setup and Tunnel Warmup

Conduct Steps III.A.1.b-f, with one exception: open the Excel template named *wall_static.xlsx* and save it with the same naming convention described previously.

2. Conduct of Testing

a. Data Collection

(1) Set the wind tunnel speed dial to the desired value.

(2) Observe the prescribed five minute stabilization time, then depress the run arrow on the front panel of the VI to collect the pressure data from the static pressure ports and pitot-static tube. Enter the file name in the pop-up dialogue box to which LabVIEW will write the data and press ‘Enter.’

(3) Perform Steps III.C.2.a.(1)-(2) until the required data sampling points have been recorded.

b. Securing the Wind Tunnel

(1) Rotate the speed dial fully counterclockwise until the indicator shows 000.

(2) Depress the red stop button labeled ‘Fan’ and the red ‘Mains Supply’ off button and ensure the green indicator lights for both functions extinguish.

c. Data Processing

(1) Transfer the data from the LabVIEW created file to the *wall_static.xlsx* template by copying and pasting. Ensure the data matrix aligns with the appropriate rows and columns in the template (Figure 33).

Temp:	56°F				
PATM:	29.97" Hg				
RH:	60%				
All channels indicate pressure in psi					
Loc	CH	Rest	500	800	1000
PST-Po	1	-0.025539	-0.009374	0.018411	0.045932
PST-p	2	-0.017408	-0.019812	-0.025102	-0.035297
pos 1	3	-0.01494	-0.022215	-0.036961	-0.051998
pos 2	4	-0.019759	-0.026059	-0.039423	-0.053073
pos 3	5	-0.022532	-0.029283	-0.043696	-0.059113
pos 4	6	-0.017161	-0.023186	-0.036148	-0.049384
pos 5	7	-0.014841	-0.01988	-0.030415	-0.041317
pos 6	8	-0.028383	-0.03449	-0.046875	-0.060293
pos 7	9	-0.020783	-0.025367	-0.035249	-0.045947
pos 8	10	-0.025051	-0.029652	-0.039366	-0.050102
windspeed (m/s)	N/A		10.83825286	22.12003739	30.20880362

Figure 33. Wall Static Pressure Template (example)

(2) Tunnel speeds are automatically determined as in Step III.A.3.b for the pitot-static tube, and the wall static pressure plot is automatically generated.

3. Wall Static Pressure Profile

The wall static pressure profile testing was conducted with three different variations: no tape installed over the vent gap after the test section and a gasket installed in the fan access cover, no tape installed over the gap and no fan access cover gasket, and with tape installed over the vent gap and no fan access cover gasket. Each of these tests were conducted at four speed dial settings: 300, 500, 800, and 1000 to determine which of the configurations provided the smoothest wall static pressure profile and the effects the physical changes had on tunnel speed.

a. Wall Static Pressure with Open Vent

Results from both series of tests with the test section open to atmospheric pressure were very similar with the static pressures averaging 10.5% higher in the test with the gasket installed in the fan access cover vs. the gasket removed. Both tests show a notch in the wall static pressure distribution at Position 5.

(1) Fan Access Cover Gasket Installed. Early in the conduct of testing, an air leak was noted from the fan access cover. Air escaped from approximately 50% of the perimeter of the cover and the leak contributed to significant noise in the wind tunnel area. A foam gasket was manufactured to seal the fan access cover to reduce the ambient noise level and potentially improve wind tunnel performance. The static pressure distribution at all four tested speeds demonstrated a similar notch in Position 5 where the wall static pressure averaged 44% higher than the average of the Positions 4 and 6 pressures, and there was an 80% increase in wall static pressure on average from the entrance to the exit of the test section (Figure 34). A second effect on the tunnel was a 20% reduction in the maximum tunnel speed as determined by both pitot-static tube and the inclined manometer, with the maximum reaching only 31.5 m/s in this test.

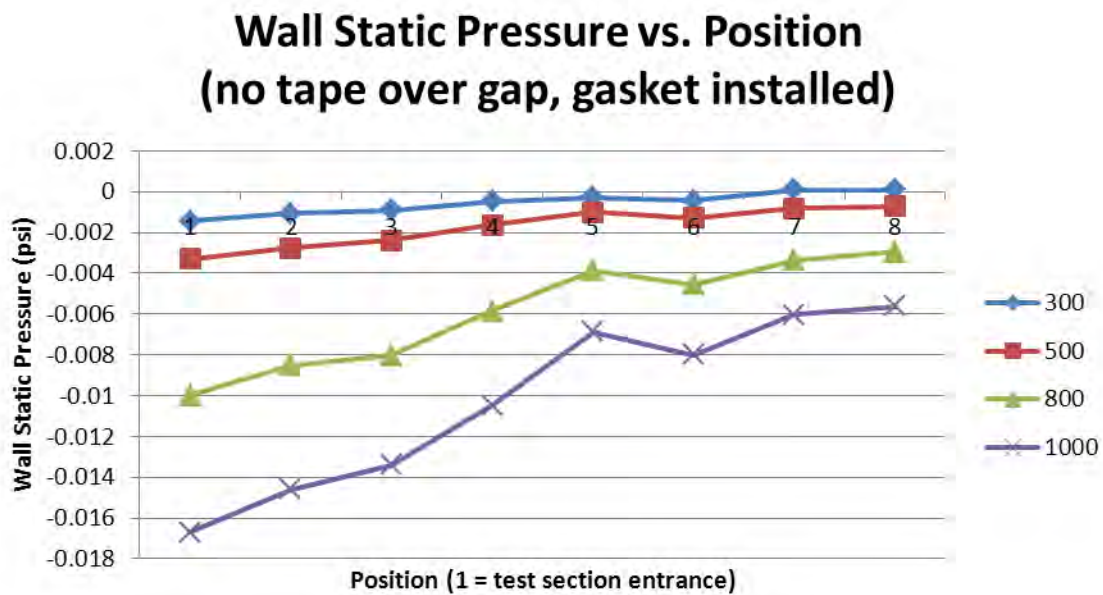


Figure 34. Wall Static Pressure, Vented Test Section, Fan Access Gasket Installed

(2) Fan Access Cover Gasket Removed. Similar to the test with a gasket in the fan access cover, the static pressure distribution at all four tested speeds again revealed a notch in Position 5 where the wall static pressure averaged 32% higher than the average of the Positions 4 and 6 pressures, while the wall static pressure rose an average of 65% across the length of the test section (Figure 35). As in the previous test, a

20% reduction in the maximum tunnel speed from the calibration test was noted with the highest recorded velocity equaling 31.3 m/s.

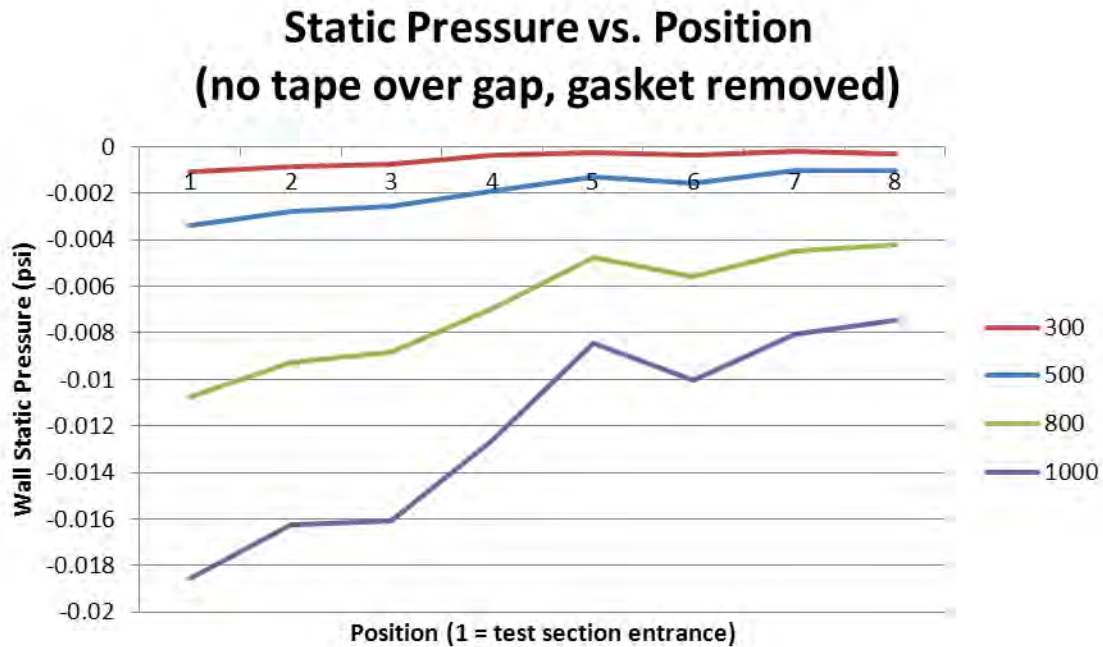


Figure 35. Wall Static Pressure, Vented Test Section, Fan Access Gasket Removed

b. Wall Static Pressure with Taped Vent

When the gap that vents the test section was sealed with tape, there were two significant effects: the wall static pressure difference from the entrance to the exit was reduced to an average increase of 12.7%, and the magnitude of the notch at Position 5 was notably diminished. The wall static pressure at Position 5 was an average of 2.5% above the mean values of Positions 5 and 6, one order of magnitude smaller than in the testing with the vent unsealed (Figure 36). Average tunnel speeds for this test were within 1% of those measured during the calibration testing, demonstrating there was no electrical or mechanical malfunction affecting the performance of the wind tunnel during the conduct of the tests with a vented test section.

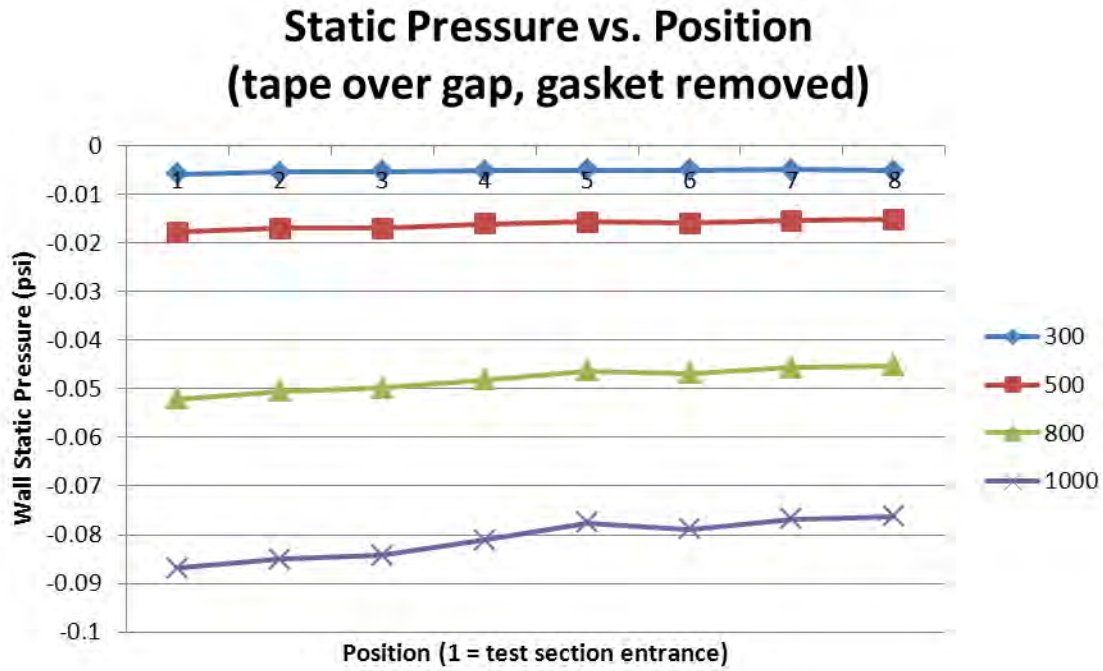


Figure 36. Wall Static Pressure, Sealed Test Section, Fan Access Gasket Removed

c. Comparison

The wall static pressure distribution at the maximum speed dial setting with the test section vent sealed with tape resulted in a smoother distribution with both the vented tests having a wall static pressure difference of 0.011067 psi across the test section, while the sealed test section pressure difference was 5% lower at 0.010548 psi (Figure 37). The differences between the wall static pressure distribution with and without the sealed vent are likely caused by the sudden expansion of the jet passing from the test section into the vented area, causing the propagation of upstream pressure effects due to the elliptical nature of the subsonic freestream flow.

Wall Static Pressure Distribution Comparison (Speed Dial = 1000)

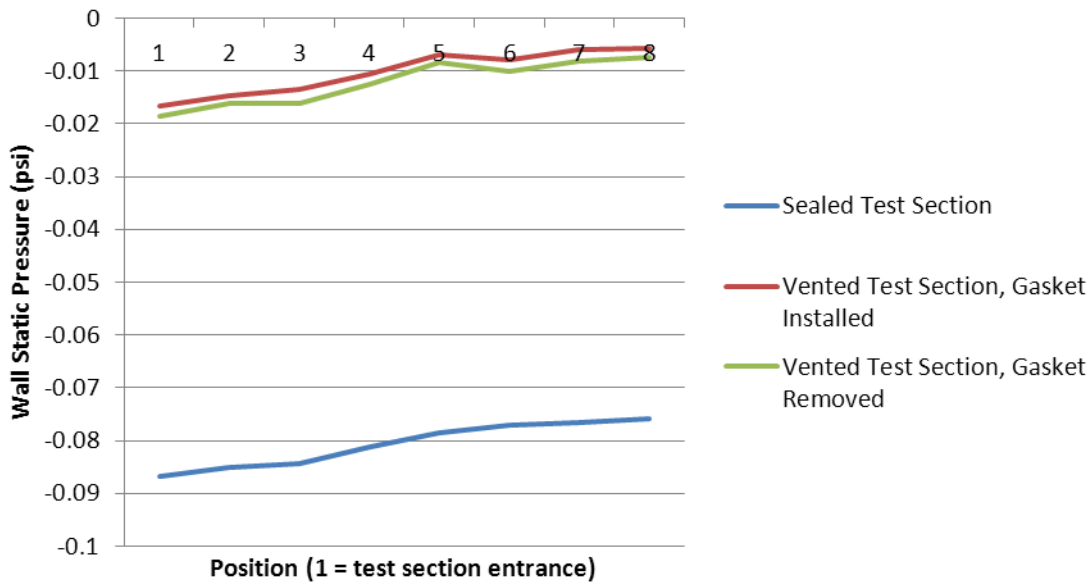


Figure 37. Wall Static Pressure Distribution Comparison

D. CTA/BOUNDARY LAYER PROBE TRAVERSAL

1. CTA Calibration²⁵

a. CTA Setup

(1) Place the function selector switch in STD. BY. and turn on the power to the CTA unit (Figure 38).

(2) Set the low pass filter to 10 kHz, the high pass filter to DC, and the gain to 1 on the signal conditioner (Figure 39)

(3) Set integration time to 0.1 seconds for channel 1 on the RMS unit, and to one second for channel 1 on the mean value unit (Figure 40).

(4) Connect a BNC cable to the PROBE BNC socket on the front of the CTA unit to the CTA probe support and probe with a four meter cable.

²⁵ DANTEC Dynamics, *56C17 Manual* (DANTEC Documentation Department, 2003), 7–9.

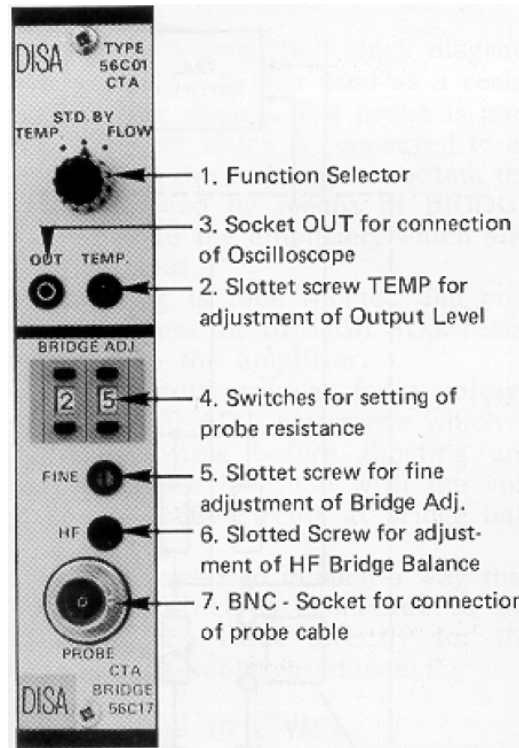


Figure 38. CTA Bridge and CTA Front Panel (From DANTEC, 2003)²⁶

²⁶ Ibid., 4.



Figure 39. CTA Signal Conditioner



Figure 40. CTA RMS and Mean Value

(5) Set the BRIDGE ADJ. switch to 00, and Turn the FINE setscrew fully counterclockwise with a flat head screwdriver.

(6) Adjust the TEMP. setscrew with a flat head screwdriver until the digital voltmeter indicates zero volts.

(7) Place the function selector switch in TEMP.

b. CTA Balancing

(1) Shift the left-hand BRIDGE ADJ. switch from zero toward nine by pressing the button below the indication until the digital voltage meter shifts from a positive value to negative (if the meter reads zero volts, continue to step III.D.1.c).

(2) Shift the left-hand switch back one number by pressing the button above the indication. The digital voltage meter should be a positive value.

(3) Shift the right-hand switch back one number by pressing the button below the indication until the digital voltage meter shows a negative value.

(4) Adjust the FINE setscrew until the digital voltage indication reads zero volts.

c. CTA Resistance Measurement

(1) Position the function selector switch to STD. BY.

(2) Remove the probe from the probe support and install the shorting probe (Model 55H30) into the probe support.

(3) Set the function selector switch to TEMP. Record the indicated voltage (V_{ind}) from the digital meter. The total resistance (R_{TOT}) of the BNC cable and CTA probe mount is determined via Equation 2.

$$R_{TOT} = 10V_{ind}$$

Equation 2

d. Overheat Selection

(1) Calculate the probe resistance (R_p) (Equation 3).

$$R_p = R_{20} [1 + \alpha_{20} (T - 20)]$$

Equation 3

Where,

R_{20} is the probe resistance at 20°C,
 α_{20} is the probe temperature coefficient of resistance,
 T is the mean operating temperature in °C, and
 R_p is the probe resistance at the operating temperature.

(2) Calculate the overheat ratio (a) (Equation 4).

$$a = \frac{R_p - R_o}{R_o}$$

Equation 4

Where,

R_p is the probe resistance at the operating temperature,
 R_o is the probe's cold resistance,
($R_o = 5 - R_L$, R_L is on probe cover), and
 a is the overheat ratio.

(3) Determine the total resistance of the probe and cabling at its operating temperature (Equation 5).

$$R_{TOT(hot)} = (1 + a) R_o + R_L + R_C$$

Equation 5

Where R_c is the cable resistance, $R_c = R_{TOT} - 5$

(4) Set the digital voltage meter using the BRIDGE ADJ. pushbuttons and the FINE setscrew to the calculated $R_{TOT(hot)}$ value.

(5) Remove the shorting probe from the probe support and install the probe into the probe support.

e. Square Wave Response Check

(1) Connect a BNC cable from the channel 1 output on the back of the CTA unit to the oscilloscope.

(2) Shift the function selector switch quickly from TEMP. to FLOW to activate the square wave generator. Position the HF ADJUST setscrew until the appropriate square wave response is displayed (Figure 41). Examples of problems in the CTA calibration are evident in the square wave response and require either rebalancing of the CTA bridge or changing the settings of the internal switches described in section II.D.5 (Figure 42).

Correct square wave test, $U = 30$ m/s

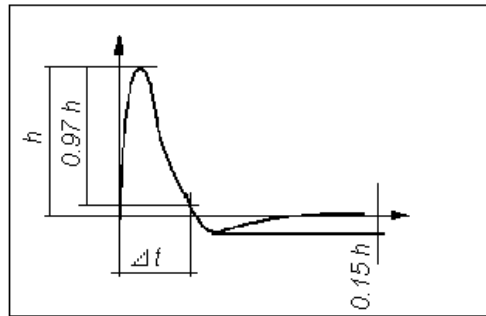


Figure 41. CTA Square Wave Response (From DANTEC, 2003)²⁷

²⁷ Ibid, 4.

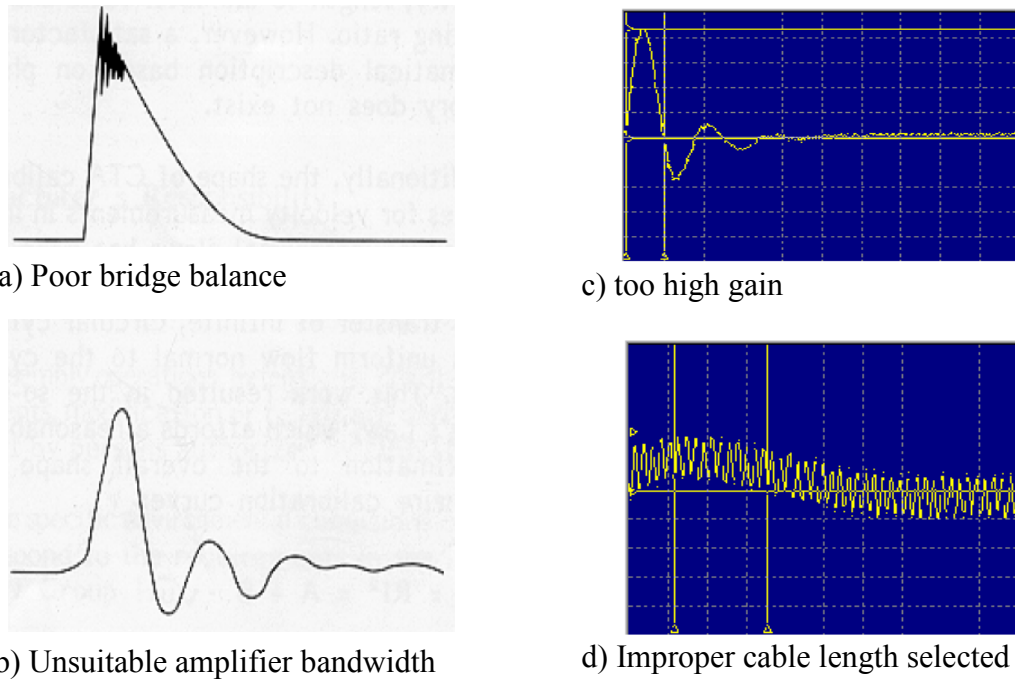


Figure 42. Incorrect CTA Square Wave Responses (After DANTEC, 2003)²⁸

(3) Secure the square wave generator by turning the function selector switch to STD. BY.

(4) Remove and store the CTA probe and shorting probe. Disconnect the probe mount from the PROBE connection on the 56C17 module.

2. Test Setup

a. Tunnel Setup

(1) Perform or verify Step III.A.1.a is completed.

(2) Install or verify installed all the wall static pressure plugs with the exception of the port the CTA lead is to pass through.

(2) Verify the bottom of the probe mount holder is higher than the top of the mounting plate to prevent any interference during traverse motor installation.

²⁸ Ibid., 9.

Reposition the carriage on the BiSlide by energizing the VP9000 controller and pressing the '+' button for Motor 1 as needed. Turn off the VP9000 controller.

(3) Mount the traverse motor in the desired position on top of the test section with the hole on the mounting plate lining up with the removed wall static plug. The second hole on the mounting plate is large enough to allow the adjacent wall static pressure plug to pass through it. Three Allen head bolts fix the mounting plate and traverse motor to the test section.

(4) Remove the operator side window from the test section.

(5) Place the empty probe mount in the test section and insert the BNC cable connector up through the vacant static pressure port. Connect the BNC cable and probe mount to the PROBE socket on the 56C17 CTA bridge.

(6) Turn on the VP9000. Depress the '-' button for Motor 1 to reposition the carriage and probe mount holder. Verify the bottom of the probe mount holder passes through the hole in the mounting plate and test section smoothly with no binding, and that the probe mount cable is not bound between the probe mount holder and the wall of the mounting plate. The probe mount holder must be inserted far enough into the test section to fit the probe mount in to place (length depends on which probe mount is used). Stop Motor 1 when the desired position is reached.

(7) Insert the probe mount through the hole on the bottom of the probe mount holder and tighten the set screw to fix the probe mount in place. Align the probe mount cable to the groove in the back side of the probe mount holder and use strips of tape to hold it in place. Install tape on the mounting plate hole to seal the gap.

(8) Install the CTA probe in the probe mount.

(9) Place the function selector switch on the 56C17 module to FLOW.

(10) Reinstall the operator side window.

b. Instrument Setup and Tunnel Warmup

Conduct Steps III.A.1.b-f, with the following exceptions:

(1) Open the Excel templates named *CTA.xlsx* and *CTA_raw_template.xlsx* and save them with the same naming convention described previously.

(2) Start the LabVIEW VIs named *PressureBrick.vi*, *dapdaq.vi*, and *Velmex.vi* (all VIs have a shortcut on the PC desktop).

(3) Depress the run button for the *dapdaq.vi*. Push the Setup DAP button.

(4) Configure the DAP for no digital inputs, one analog input, a sampling frequency of 20,000 kHz, the number of samples as 100,000 (five seconds of data), and check the box for calculating the mean and standard deviation as shown (Figure 43).

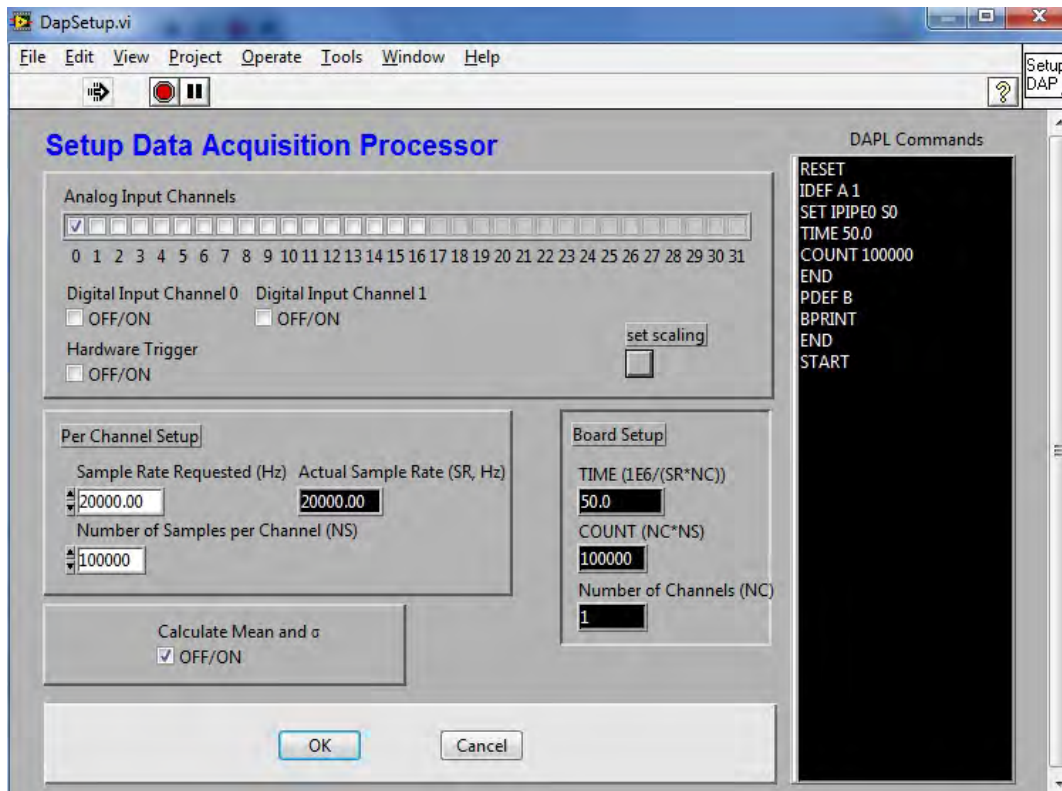


Figure 43. DAP Setup

(5) Read and record the values for the low pass filter, high pass filter, and sampling frequency in the *CTA.xlsx* template.

(6) Position the CTA in the center of the test section using the VP9000 Motor 1 controller.

3. CTA Calibration Coefficient Determination

a. Data Collection

(1) Set the wind tunnel speed dial to 300.

(2) Observe the prescribed five minute stabilization time, then depress the run arrow on the front panel of *PressureBrick.vi* to collect the pressure data from the pitot-static tube. Enter the file name in the pop-up dialogue box to which LabVIEW will write the data and press 'Enter.'

(3) Press the Take Data button on the *dapdaq.vi* and ensure the 'Data Acquired' light turns green (Figure 44).

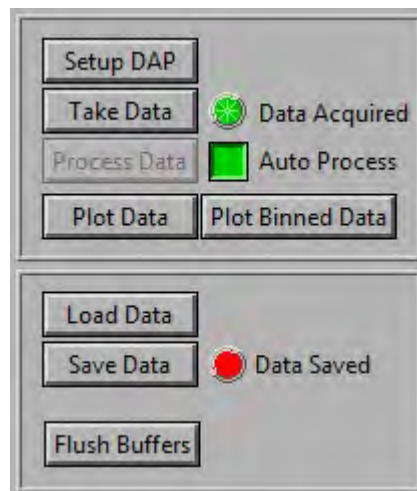


Figure 44. DAP Data Acquired

(4) Press the Save Data button. On the pop-up screen select Unsteady Data and press save. Save the data in the format tunnel speed Excel file (e.g. *300.xlsx*) for temporary storage until the test is completed. Verify the Data Saved light

turns green (Figure 45). The VI will remind the operator to save data if a successful save does not occur before pressing the Take Data button again.

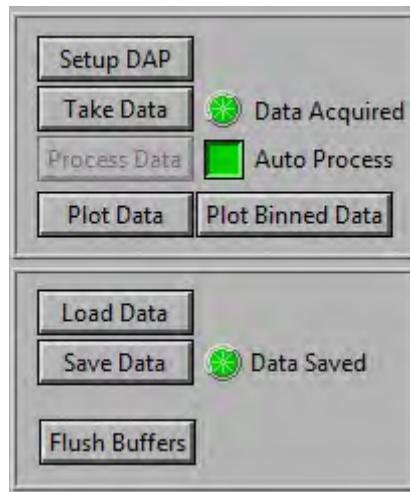


Figure 45. DAP Data Saved

(5) Increase the wind tunnel speed by rotating the speed dial clockwise by an increment of 50.

(6) Repeat Steps III.D.3.a.(2)-(5) until a measurement at a speed dial setting of 1000 is completed.

(7) In the pink command entry box in the *Velmex.vi* enter the command 'I1, M45320, R' to position the CTA probe 2 mm from the top of the test section for the boundary layer mapping (Figure 46).

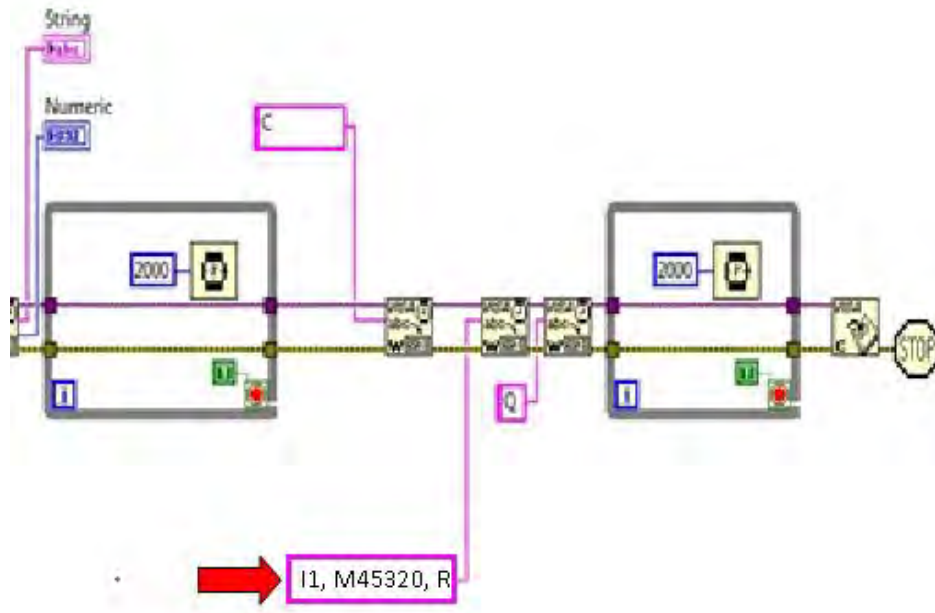


Figure 46. Velmex Command Entry for Boundary Layer Initial Conditions

b. Data Processing

(1) Save the pitot-static tube pressure data into the *CTA.xlsx* file. The tunnel speed (U_∞) is automatically calculated per Step III.A.3.b.

(2) Save the CTA voltage data from each iteration into the *CTA_Raw_template.xlsx* file. The mean and standard deviations are automatically calculated.

(3) Transfer the voltage (E) mean and standard deviation into the *CTA.xlsx* file in the appropriate rows. The values of E^2 and \sqrt{U} are calculated automatically. Two plots are generated (Figures 47 and 48). The linear curve fit coefficients must be entered into the CTA determined velocity (U_{CTA}) calculation equation, e.g. $[(E^2 - 0.505)/1.644][(E^2 - 0.505)/1.644]$ from Figure 48. The mathematical difference and percent difference from the PST velocity is calculated automatically.

Voltage vs. Wind Speed

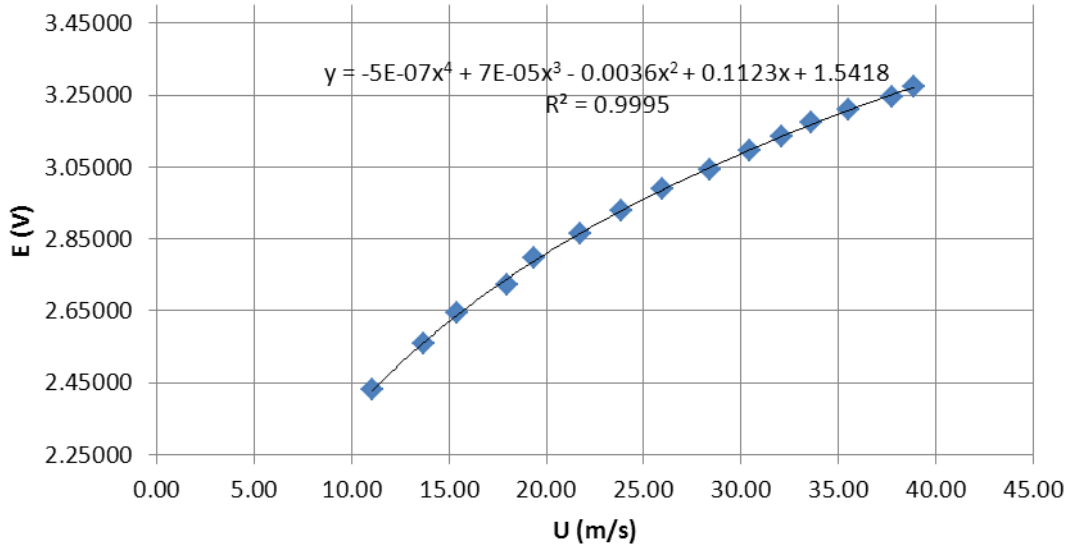


Figure 47. CTA Plot (E vs U)

Linearized Hotwire Calib Curve: E^2 vs \sqrt{U}

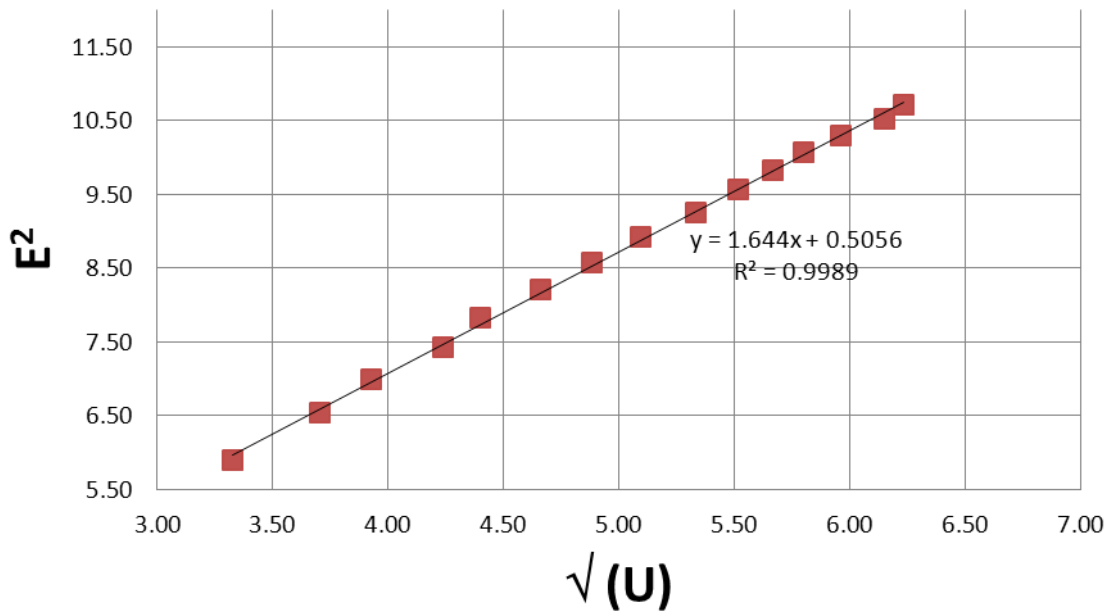


Figure 48. CTA Linearized Calibration Plot (E^2 vs \sqrt{U})

4. Boundary Layer Measurement

The wind tunnel is still operating at the desired speed with the hotwire 2 mm from the top wall of the test section.

a. Data Collection

(1) Wait five minutes. Press the Take Data button on the *dapdaq.vi* and ensure the 'Data Acquired' light turns green (Figure 44).

(2) Press the Save Data button. On the pop-up screen select Unsteady Data and press save. Save the data in the format tunnel speed Excel file (e.g. *300.xlsx*) for temporary storage until the test is completed. Verify the Data Saved light turns green (Figure 45). The VI will remind the operator to save data if a successful save does not occur before pressing the Take Data button again.

(3) In the pink command entry box in the *Velmex.vi* enter the command 'I1, M-#, R' traverse the hotwire the desired '#' of steps in the downward direction (Figure 46). Note that 200 steps = 1 mm.

(4) Save the CTA voltage data into the *CTA_raw_template.xlsx* template and save the file using the naming convention previously discussed. Transfer the mean voltage and standard deviation data to the *CTA_template.xlsx* file. The distance from the test section wall is plotted against U_{CTA} .

(5) Repeat Steps III.D.4.a.(1)-(4) until U_{CTA} levels off, with both U_{CTA} and turbulence intensity approaching the freestream values determined in the calibration procedure (Step III.D.3.b.(3)).

(6) Repeat Steps III.D.4.a.(1)-(4) until U_{CTA} levels off, with both U_{CTA} and turbulence intensity approaching the freestream values determined in the calibration procedure (Step III.D.3.b.(3)).

b. Data Processing

(1) The value of the boundary layer thickness (δ) is taken from the distance from the wall where U_{CTA} changes by less than 1% between samples after the plot has leveled near freestream velocity ($U_{CTA} \approx 0.99U_\infty$).

(2) The displacement thickness (δ^*) is calculated using Equation 6.

$$\delta^* = \int_0^{y \rightarrow \infty} \left(1 - \frac{U_{CTA}}{U_\infty}\right) dy$$

Equation 6 Displacement Thickness²⁹

(3) The momentum thickness (θ) is calculated using Equation 7.

$$\theta = \int_0^{y \rightarrow \infty} \frac{U_{CTA}}{U_\infty} \left(1 - \frac{U_{CTA}}{U_\infty}\right) dy$$

Equation 7 Momentum Thickness³⁰

(4) The shape factor (H) is calculated using Equation 8.

$$H = \frac{\delta^*}{\theta}$$

Equation 8 Shape Factor³¹

5. CTA Calibration Verification

a. Data Collection

(1) Position the hotwire on the centerline of the test section.

(2) Repeat Steps III.D.3.a.(1)-(6), increasing the speed dial setting by increments of 100 vice 50 for the post-test check.

²⁹ Muguru Chandrasekhara, *ME-4220 Course Notes*, 2009, 58.

³⁰ *Ibid.*, 59.

³¹ *Ibid.*, 60.

b. Securing the Wind Tunnel

(1) Rotate the speed dial fully counterclockwise until the indicator shows 000.

(2) Depress the red stop button labeled ‘Fan’ and the red ‘Mains Supply’ off button and ensure the green indicator lights for both functions extinguish.

(3) Position the CTA function selector switch unit to STD. BY.

c. Data Processing

(1) Repeat Steps III.D.3.b.(1)-(3).

(2) Evaluate the two generated plots to determine if the calibration conducted in Step III.D.3 remains valid by comparing the shape of the curves and the coefficients of the linear curve fit.

6. CTA Test Results

Testing performed with the CTA was conducted with the parameters described in the preceding procedure in both the freestream and the boundary layer. For all the analyses except spectral density, the data was condensed from 10^5 points to a mean and standard deviation from which U_{CTA} , one-dimensional turbulence intensity, and boundary layer characteristics.

a. CTA Velocity

The CTA velocities averaged within 2.5% of the PST determined velocities, with the highest difference in the velocities occurring in the post test verification runs with an average difference between calculated velocities of 3.8%, demonstrating a high confidence in the reliability of the CTA calibration when the tunnel is properly warmed up (Figure 49). This is a stark contrast to the average difference of 12% between these velocities when the tunnel was warmed up for only 20 minutes (Figure 50). The flattening of the curve as \sqrt{U} increases is probably due to the reduced heat transfer as the air temperature in the tunnel rises closer to the temperature of the

hotwire filament, providing a falsely low voltage to maintain the constant temperature of the CTA. This is also evident in the post test verification check where the temperature in the tunnel had stabilized at a higher temperature, resulting in a lower voltage over the range of \sqrt{U} and demonstrates the proper linear relationship.

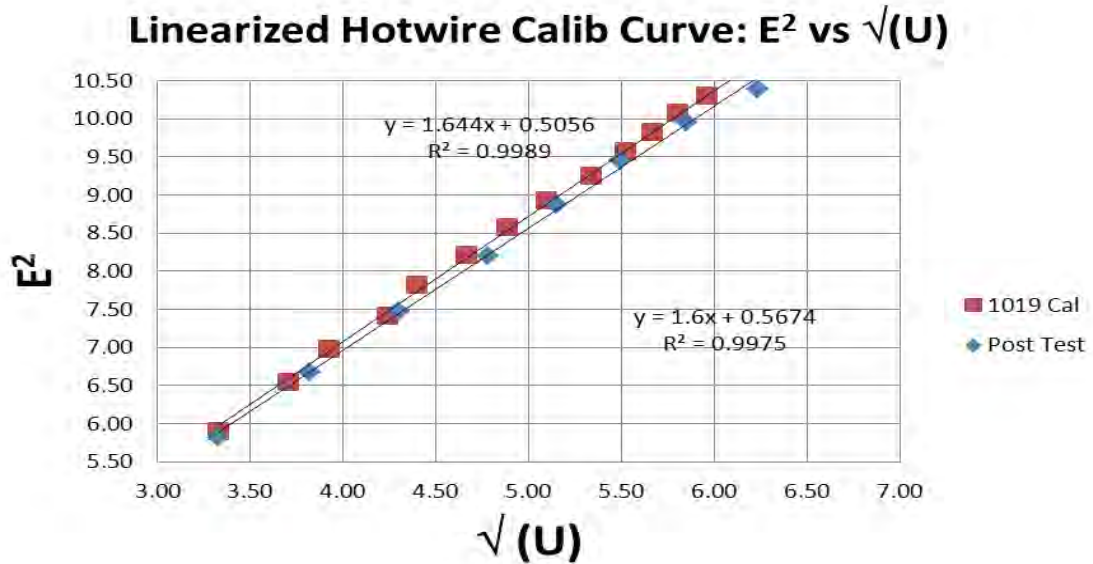


Figure 49. CTA Post Test Comparison with 60 Minute Tunnel Warm-up

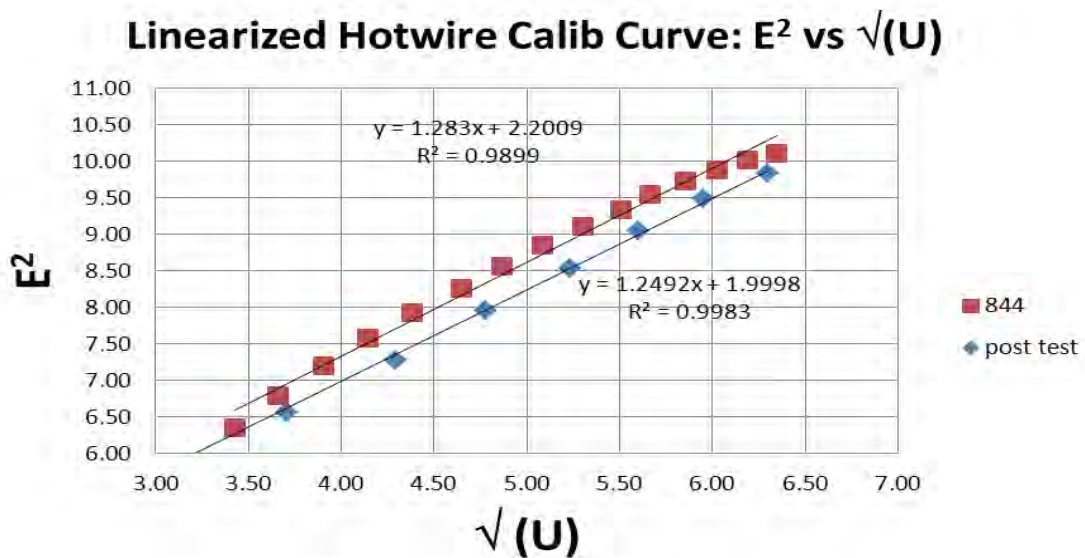


Figure 50. CTA Post Test Comparison with Insufficient Tunnel Warm-up

b. Turbulence Intensity

The turbulence intensity (I) in the wind tunnel is a measurement of the fluctuations in the fluid flow within the test section, expressed as a percent. The tunnel speed was calculated from the CTA data using the method described in III.D.3.b.(3). From the calculated velocities, the one-dimensional turbulence intensity could be determined (Equation 9).

$$I = u' / U_{\infty}$$

Equation 9 Turbulence Intensity³²

Where,

u' is the turbulent velocity fluctuation standard deviation, and
 U_{∞} is the freestream velocity at the same location.

slightly higher than that expected of most research wind tunnels. However, this is within the accepted range of most applied aerodynamics test facilities. The turbulence intensity is highest at a tunnel speed near 13 m/s, however, the accuracy of tunnel speed measurements at low speed dial settings are less accurate than at higher speeds. Over the tunnel speed range of 16–25 m/s, the turbulence intensity drops below 0.06%, raising the possibility of conducting boundary layer transition characteristics in this range. The turbulence intensity rises again from 25–38 m/s with a maximum of 0.17% at a tunnel speed near 34 m/s (Figure 51). A possible resonance speed in the wind tunnel may be contributing to the turbulence intensity at speed dial settings from 850–900 as evidenced by a significant vibration and loud humming noise detected while the tunnel is operated through this speed range.

³² Gilder Nader, Claudia dos Santos, Paulo Jabardo, Monica Cardoso, Nilson Taira, and Marcos Pereira, *Characterization of Low Turbulence Wind Tunnel* (Institute for Technological Research, 2006), 2.

Average Turbulence Intensity vs. Speed Dial Position

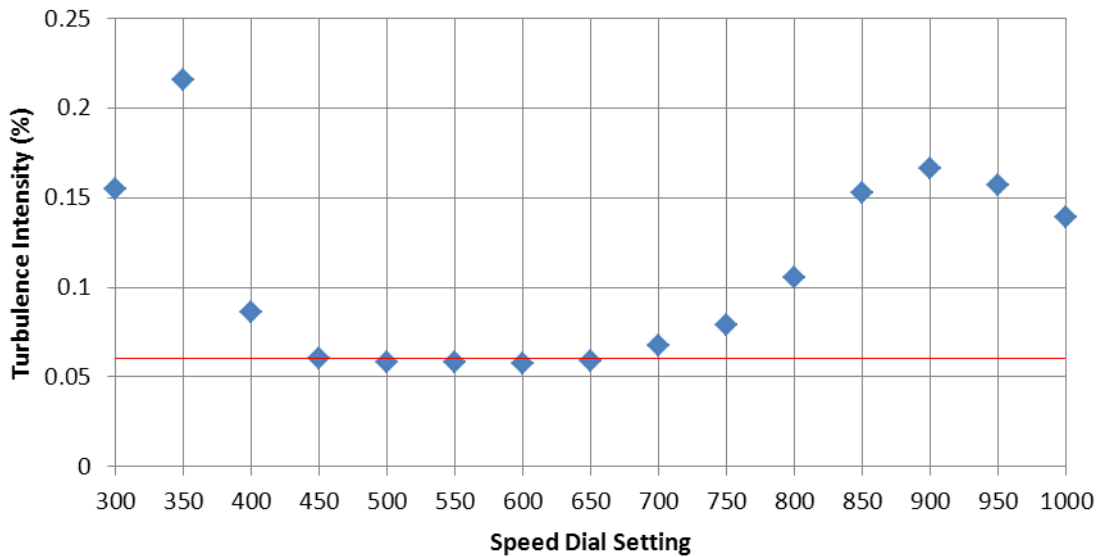


Figure 51. Average Tunnel Turbulence Intensity

c. Boundary Layer

The boundary layer measurements within the test section resulted in a 3mm thickness at the first data point and exhibited parabolic growth to 23mm at 86% of the test section length. The relationship between the turbulent boundary layer thickness and the displacement thickness ($\delta^* = \delta/8$) is nearly demonstrated, with a 29% difference from this relationship. Neglecting the first data point (where the first sample was near the boundary layer thickness), the relationship is followed more closely with only an 8.9% difference between the experimentally determined displacement thickness and that of the 1/8 relationship (Figure 52) with a shape factor of 1.12, a 14% difference from the shape factor of 1.3 for turbulent flows.³³ Note that the growth of the boundary layer and the displacement thickness will cause an apparent constriction to the freestream flow resulting in the acceleration of the air in the test section as the cross-sectional area

³³ Ibid., 133.

remains constant. No corrections for the displacement thickness effects on U_∞ have been evaluated or applied during the conduct of these experiments.

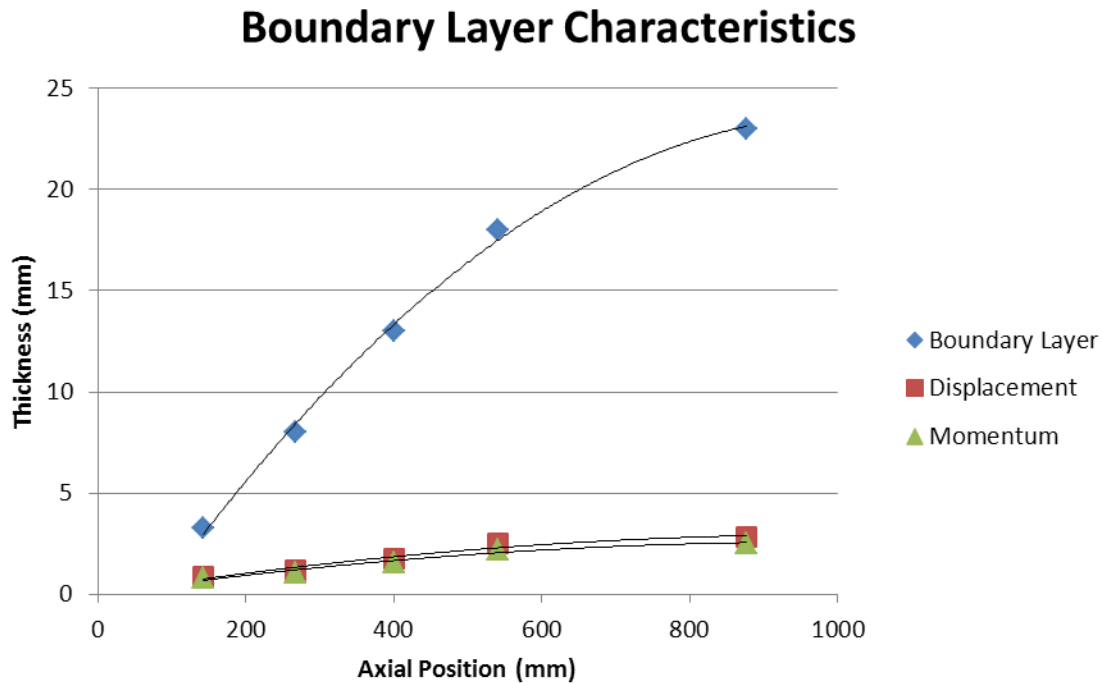


Figure 52. Boundary Layer Profile

d. Spectral Density

(1) The spectral density function for MATLAB was used to evaluate the spectrum for a known amplitude sine wave to verify proper operation of the code. A function generator was used to produce a 1V, 100 Hz sine wave that was sampled at 200 Hz for 5 seconds. The spectral density function was used to create a spectral density plot from the raw data and resulted in the appropriate frequency peak near 100 Hz and an integrated area of 0.711 V^2 , less than a 1% difference from the expected value of 0.707 V^2 . Two reasons for the deviation are that the sine wave generated by the function generator was not precisely 100 Hz, nor was the amplitude exactly 1 V, resulting in some error in the spectral density function output (Figure 53). Thus, it was concluded that the spectra were computed accurately.

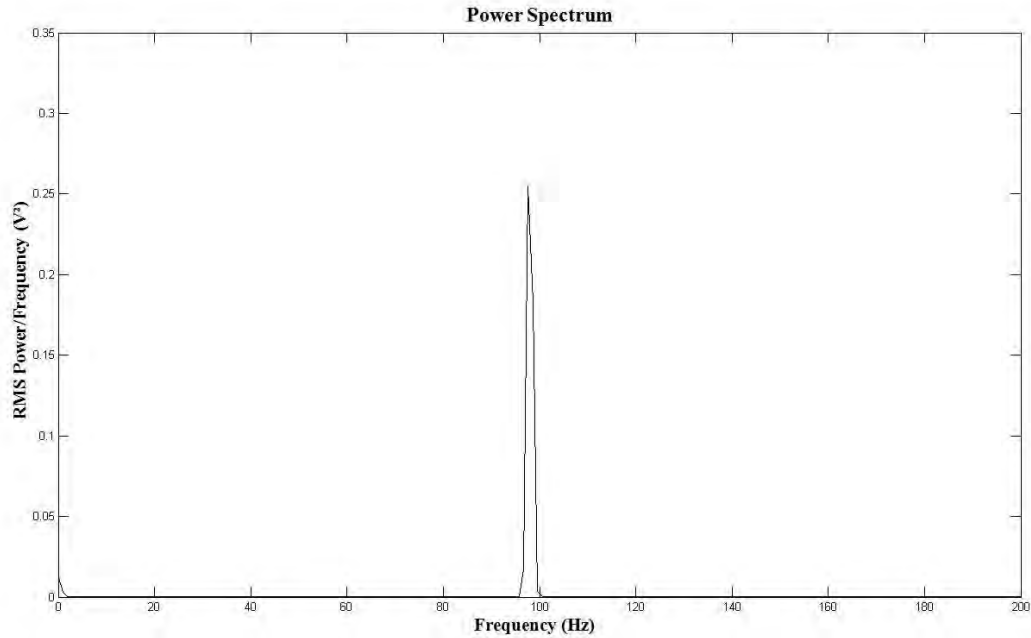


Figure 53. Sine Wave Spectral Density

(2) A spectral density evaluation was conducted on the freestream velocity at the centerline of the test section with the $U_\infty \approx 38.5$ m/s using the *PSPECTRA.m* function described in Section II.F.4. Each sample consisted of 100,000 samples collected at a sampling frequency of 20,000 Hz, satisfying the Nyquist frequency requirement with the CTA low pass filter set at 10,000 kHz. The samples were rearranged into blocks of 1,024 samples with an equal number of zeroes added for increased resolution of the fast fourier transform. The result shows the mean-squared amplitude of the turbulence in the freestream velocity signal (Figure 54). The low frequency activity may be due to Nyquist noise; even with the conditioned power supply used in the laboratory, noise may be present in the CTA electronics, however, the levels are very small and are not a cause for any concern. The high frequency oscillations may be evidence of the breakdown of small vortices within the flow as they decay from viscous effects. The use of a tachometer for either motor speed or fan blade count measurement could provide additional information in looking for their possible contribution to the peaks demonstrated within the spectrum.

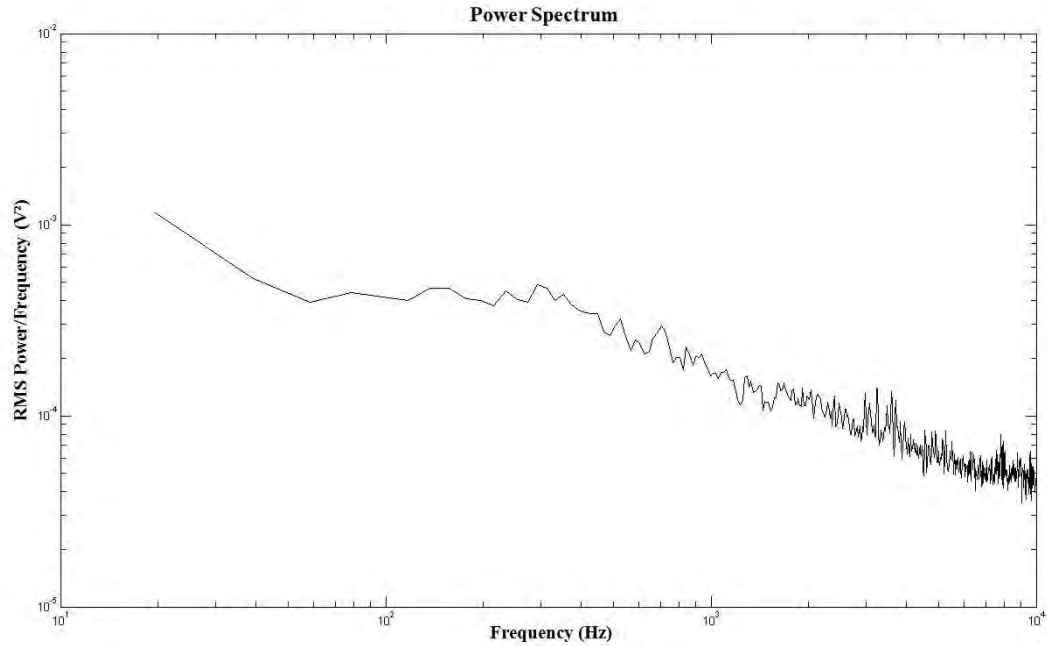


Figure 54. Freestream Spectral Density

(3) The spectral density was calculated in the boundary layer at a distance of 2 mm from the tunnel wall with $U_{\infty} \approx 38.5$ m/s using the same process described in III.D.6.d.(2) (Figure 55). The spectral density demonstrates similar characteristics of a fully developed turbulent boundary layer over a flat-plate. The low frequency (small wave number) end of the spectrum indicates high energy due to it being the energy containing range, with a very well defined inertial sub-range (as demonstrated by the $-5/3$ slope line) and attenuation of the energy at the high frequency, indicating that the turbulence is in near equilibrium in the wall boundary layer. That the spectrum spans over five decades on the ordinate confirms its determination has been quite accurate, with a good signal-to-noise ratio.

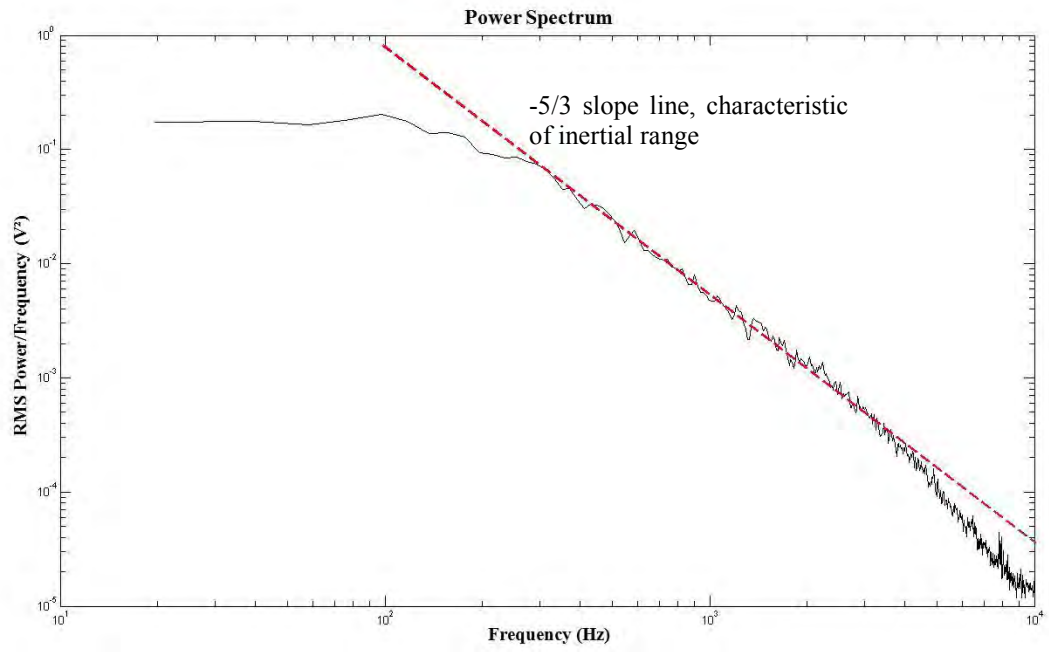


Figure 55. Boundary Layer Spectral Density (2mm from wall)

THIS PAGE INTENTIONALLY LEFT BLANK

IV. CONCLUDING REMARKS AND RECOMMENDATIONS

A. REMARKS

1. Velocity Characteristics

The MAE wind tunnel has been reassembled, instrumented, and its flow characteristics evaluated. The maximum achievable freestream tunnel speed was determined to be 37.5 m/s at a turbulence intensity of 0.11% at the tunnel centerline. The flow uniformity was determined to be within $\pm 7.5\%$ of the mean freestream velocity, with the lower half of the test section along the spanwise centerline showing a more pronounced difference. The cause of the velocity non-uniformity and the 16% reduction in the rated speed of the tunnel are likely attributable to multiple performance affecting components, such as small misalignments of multiple section flanges, several air leaks from both flanges and the fan access cover, and the unknown condition of the mesh screens in the tunnel. It is not possible to determine the exact causes for the observed variation since many parameters such as the porosity of the screens or its potential influence on flow instabilities in the test section are not well documented. Literature reviews indicate that this factor may be contributing to the greater than normal velocity field differences in the test section beyond that of most general purpose tunnels.³⁴

2. Turbulence Intensity

The average turbulence intensity in the MAE wind tunnel is 0.11%. Thus, this tunnel is well suited for applied aerodynamics studies. For research on flows that are sensitive to turbulence intensity such as boundary layer transition, significant flow improvements need to be made prior to using this facility.

3. Boundary Layer Characteristics

The test section boundary layer exhibits typical equilibrium turbulent energy spectrum behavior, and the boundary layer shows normal growth over the length of the

³⁴ Jewel Barlow, William Rae, and Alan Pope, *Low-Speed Wind Tunnel Testing* (Wiley-Interscience, 1999), 90–94, 124.

test section. However, the shape factor within the boundary layer is lower than that of a fully developed turbulent boundary layer at a value of 1.13. This difference may, in part, be due to the measurement in the region of the test section wall where, since the static pressure port was removed to accommodate the hotwire probe and its mount, a small cavity was present. Future flat-plate testing is planned to evaluate its boundary layer characteristics with the eventual goal of reducing its drag coefficient.

B. RECOMMENDATIONS

1. Wind Tunnel Disassembly

Investigation of the mesh screens, turning vanes, and honeycombs requires the re-assembly of the wind tunnel. This would allow rectification of any equipment that may need refurbishment and make them acceptable for fundamental research. The re-assembly would also enable properly aligning of the flanges, and would allow personnel to inspect and smooth any irregularities on the internal flange joints or tunnel walls.

2. Conduct of Testing

Based on the testing conducted over the course of this thesis, the following details should be observed when operating the wind tunnel:

- Fan Access Cover gasket should not be installed until tunnel inspection is completed.
- The tape sealing the breather gap should remain installed to provide the smoothest wall static pressure profile possible and maximize achievable tunnel velocity.
- Use a speed dial setting of 300 as a minimum; velocity measurements via PST are inconsistent at speed dial settings below this mark.
- The wind tunnel should be operated for a minimum of one hour at maximum speed for warm-up to minimize the effects of freestream temperature variations on CTA and pressure transducer measurements.

C. CONCLUSION

The NPS MAE wind tunnel requires further investigation into the flow uniformity within the test section. While the 2-D uniformity showed a $\pm 7\%$ velocity deviation using the pressure rake, a vertical traverse down the centerline of the test section using the boundary layer probe and CTA showed a velocity deviation of $\pm 5\%$ and $\pm 3.6\%$, respectively, suggesting the flow uniformity determined from the pressure rake is inflated. A 2-D map of the velocity field using CTA measurements are needed to verify the flow quality of the wind tunnel is satisfactory for applied, low speed aerodynamic research. The instrumentation, data acquisition system, and data processing software has been tested and the MAE wind tunnel system is ready for use as a laboratory facility for the faculty and students at NPS or other interested DoD organizations.

THIS PAGE INTENTIONALLY LEFT BLANK

BIBLIOGRAPHY

- Barlow, Jewel B., William H. Rae, and Alan Pope. *Low-Speed Wind Tunnel Testing*. New York, New York: John Wiley & Sons, Inc., 1999.
- Chandrasekhara, M. S. "ME-4220 Course Notes." Monterey: Chandrasekhara, September 24, 2009.
- DANTEC Documentation Department. *56C17 Manual*. Skovlunde: DANTEC Documentation Department, 2003.
- Krauss, Thomas P., Loren Shure, and John N. Little. *Signal Processing Toolbox for Use with MATLAB*. Natick, Massachusetts: The MathWorks, Inc., 1993.
- Microstar Laboratories, Inc. *DAP 5200a Manual*. Bellevue, Washington: Microstar Laboratories, 2001.
- . *Microstar DAPL Operating System*. September 7, 2011. http://www.mstarlabs.com/software/dapl/tabs.html#_overview, (accessed September 7, 2011).
- . *Mstar Labs DAP 5200a Sample System Drawing*. September 6, 2011. <http://www.mstarlabs.com/dataacquisition/graphics/dap5200adrawing.html>, (accessed September 6, 2011).
- . *MSXB 038 Accessory Board Manual*. Bellevue, Washington: Microstar Laboratories, Inc., 2003.
- MKS Instruments. *700 Series Baratron Pressure Transducers*. Andover: MKS Instruments, 1999.
- . *MKS Baratron Type 223B Pressure Transducer*. Andover: MKS Instruments, 1996.
- . *PR 4000 F Instruction Manual*. Andover, Massachusetts: MKS Instruments, 2000.
- Nader, Gilder, dos Santos, Claudia, Jabardo, Paulo J. S., Cardoso, Monica, Taira, Nilson M., Pereira, Marcos T. *Characterization of Low Speed Wind Tunnel*. Sao Paulo: Institute for Technological Research, 2006.
- National Aeronautics and Space Administration. September 19, 2011. <http://www.grc.nasa.gov/WWW/k-12/airplane/isentrop.html>, (accessed September 19, 2011).

Scanivalve Corporation. "Scanivalve Corp. Digital Pressure Measurement." *Scanivalve Corp.* February 8, 2007.

http://www.instrumentation.it/main/pdf/scanivalve/prod_dsa-3217_18_0311_ID.pdf (accessed September 6, 2011).

Schlichting, H., and K. Gersten. *Boundary-Layer Theory*. 8th Edition. New York, New York: Springer Publishing Company, 2000.

United Sensor Corporation. "Boundary Layer Probe." *BR-025-25-C-23-120*. Amherst, New Hampshire: United Sensor Corporation, 2011. 1.

Velmex, Inc. *Velmex BiSlide Assemblies*. http://www.velmex.com/bislide/motor_bislide.-html, (accessed September 6, 2011).

LIST OF REFERENCES

- Barlow, Jewel B., William H. Rae, and Alan Pope. *Low-Speed Wind Tunnel Testing*. New York, New York: John Wiley & Sons, Inc., 1999.
- Johnson, Gary W. *LabVIEW Graphical Programming: Practical Applications in Instrumentation and Control*. New York, New York: McGraw-Hill, Inc., 1994.
- Krauss, Thomas P., Loren Shure, and John N. Little. *Signal Processing Toolbox for Use with MATLAB*. Natick, Massachusetts: The MathWorks, Inc., 1993.
- Mehta, R.D., and P. Bradshaw. "Design Rules for Small Low Speed Wind Tunnels." *The Aeronautical Journal of the Royal Aeronautical Society*, 1979: 443–449.
- National Instruments. *Introduction to LabVIEW and Computer-Based Measurements*. Austin, Texas: National Instruments, 2010.
- Yajnik, K.S. and M. Acharya. *Proc. Symp. Turbulence: Structure and Mechanisms of Turbulence*, Vol. 1. Berlin, Germany, 1977.

THIS PAGE INTENTIONALLY LEFT BLANK

INITIAL DISTRIBUTION LIST

1. Defense Technical Information Center
Ft. Belvoir, Virginia
2. Dudley Knox Library
Naval Postgraduate School
Monterey, California
3. Professor M. Chandrasekhara
Naval Postgraduate School
Monterey, California
4. LT Scott Harvey
United States Navy
Conway, Arkansas